Ref.TH.1903-CERN

REGGEOMETRY

J.P. Ader and R. Peschanski
CERN - Geneva

R. Lacaze
Université de Genève, Département de Physique Théorique

G. Cohen-Tannoudji and C. Gilain
CEN Saclay, Service de Physique Théorique

A B S T R A C T

We propose a few general empirical laws summarizing our knowledge on two-body hadronic amplitudes. These systematics lead to a simple analytic parametrization of these amplitudes, allowing the reproduction of all the prominent features of the non-vacuum exchange data from 6 to 50 GeV/c. The obtained results, and in particular the ability of describing in a consistent way both meson and baryon exchanges, are encouraging and suggest that a framework may be found for new dynamical approaches.

Ref.TH.1903-CERN
31 July 1974

1. INTRODUCTION

The situation of two-body phenomenology is far from being entirely satisfactory. One cannot say that a unique well-determined phenomenology may exist which would permit describing all the existing data about high-energy, near forward and backward two-body and quasi-two-body scattering. All the existing models (including the elaborate Regge cut models[1]) encounter some difficulties in describing some amplitudes or categories of amplitudes.

What we intend to do here, is not to try to improve such or such a model, but to make a balance of all that has been learnt from phenomenology and amplitude analysis. We extract from the available information some general empirical laws leading to systematics of two-body reactions. By this, we mean a parametrization of non-Pomeron exchange scattering amplitudes which is universal, simple, and able to fit the data with enough accuracy. The comparison of the analytic form of our amplitudes with the one obtained in dynamical models should allow the pointing out of the difficulties of these models, and perhaps a better theoretical understanding.

We first show the derivation of the parametrization (Section 2) then apply the systematics to ρ, A_2, N_α, and Δ_δ exchanges (Section 3), and finally discuss the results, pointing out the open problems (Section 4).

2. DERIVATION

In order to derive the empirical laws which define our systematics, we first have to analyse what has been learnt (for sure) from all the attempts to describe the data.

2.1 General statements from the current models

2.1.1 Regge rules have something to do with the scattering amplitudes

The energy dependence, the phase, the position of the zeros are well described (in a first approximation) in terms of Regge pole exchanges. Such a statement is particularly well established by a few experimental analyses [$\alpha_{eff}(t)$ for ρ exchange in $\pi^- p \to \pi^0 n$ [2], high-energy behaviour of $\sigma^T_{p\bar{p}} - \sigma^T_{pp}$, $\sigma^T_{K^-p} - \sigma^T_{K^+p}$, $\sigma^T_{\pi^-p} - \sigma^T_{\pi^+p}$ [3], mirror symmetry zeros of $\pi^\pm p$ elastic polarizations, ...].

2.1.2 Exchange degeneracy is a good first approximation

The position of resonances on the Chew-Frautschi plot and the approximate flatness of exotic cross-sections implies exchange degeneracy of Regge trajectories and residues as a good first approximation. Indeed there exists strong evidence of violation of exchange degeneracy, but qualitatively one can say that exchange degeneracy is a symmetry law for the Regge pole contribution.

2.1.3 Corrections to Regge pole exchanges are necessary

The conspiracy problem in pion exchange, the cross-over phenomenon, the non-vanishing of πN charge exchange polarization, are well-known indications of the necessity of correction to Regge pole exchange, including corrections to describe the breaking of exchange degeneracy.

2.1.4 The existing models are not entirely satisfactory

The models which introduce corrections to Regge pole exchange (essentially the models based on absorptive cuts) all encounter some difficulty somewhere. Sometimes these difficulties can be overcome through some improvement of the model (e.g. introduction of secondary cuts like in the RPR model[1] to explain the πN charge exchange polarization puzzle). Other difficulties seem very severe like the persistence of shrinkage at large t for ρ exchange, whereas all the cut models predict essentially no shrinkage[4]. Another puzzling question concerns the strength of the correction according to the amplitude in which it is applied: it seems, for instance, that in absorption models the spin-flip contribution of the ρ Regge pole is too much corrected, whereas the exchange degeneracy breaking corrections are too small in high helicity flip amplitudes[5].

2.2 Dominant features of two-body amplitudes

Amplitude analyses allow the extraction of some rather model-independent information from data, which we now try to summarize.

2.2.1 s-channel helicity amplitudes have simple dynamical features

In order to detect general features of high-energy scattering, s-channel helicity amplitudes seem to be the most suitable ones. In particular the zeros, which are one of the most characteristic properties, can well be

classified according to the net s-channel helicity flip $n = |\lambda_i - \lambda_f|$. These zeros appear to be, in general, at some values of t (close to the real axis) which do not depend on the energy (or depend very slowly). As examples of these zeros let us quote:

- the cross-over zero in the non-flip vector exchange around $t \simeq -0.2$ [6];
- the near backward zero in the non-flip N_α exchange at $u' = u - u_{min} \simeq -0.2$ [7];
- the zero at $t \sim 0.6$ in the ρ flip amplitude[8];
- a possible zero at $t \sim -1.1$ in the A_2 flip amplitude[9];
- a possible zero at $u' = u - u_{min} \sim -1$ in A exchange from dip in backward $\pi^- p$ differential cross-section[10].

2.2.2 Zeros of the amplitudes

It has been remarked since a long time that the properties of these zeros lead to a geometrical interpretation for their appearance. First of all, it is remarkable that they coincide with the first zeros of Bessel functions $J_n(R\sqrt{-t})$ where R is approximately equal to 1 fermi (see Table 1). This coincidence strongly suggests that the impact parameter representation is well suited to find simple properties:

$$M_n(s,t) = 2q^2 \int_0^\infty b\,db\, J_n(b\sqrt{-t'})\, \tilde{M}_n(s,b) \qquad (1a)$$

$$\tilde{M}_n(s,b) = \frac{1}{2q^2} \int_0^\infty \sqrt{-t'}\, d\sqrt{-t'}\, J_n(b\sqrt{-t'})\, M_n(s,t) \qquad (1b)$$

where $t' = t - t_{min}$ and q is the c.m. momentum. These relations which are nothing but two-dimensional Fourier transforms in the transverse plane, approximate, in the semi-classical approximation limit, the partial wave expansion (1a) and inversion (1b).

The geometrical properties of the zeros of the amplitudes are translated into simple properties of the profile functions $\tilde{M}_n(s,b)$ which are supposed to describe the "geometry", or the distribution of matter in the interacting particles. We know, at least, two simple geometries which imply zeros analogous to the observed ones:

a) the "δ" geometry or "ring" geometry

$$\tilde{M}_n(s,b) \propto b^n\, \delta(b^2 - R^2) \Rightarrow M_n(s,t) \propto J_n(R\sqrt{-t'}) \qquad (2a)$$

b) the "Θ" geometry or "disk" geometry

$$\tilde{M}_n(s,b) \propto b^n \theta(b^2 - R^2) \Rightarrow M_n(s,t) \propto \frac{J_{n+1}(R\sqrt{-t})}{R\sqrt{-t}} \quad (2b)$$

These two forms exhibit an important property: one given geometry leads to a series of zeros varying with n, whereas the geometry is entirely described by a helicity independent distribution.

We note that the factor b^n in (2b) is essential in the definition of the profile function in order to get the corresponding form $M_n(s,b)$. It is a purely kinematical factor, completely analogous to the $\sqrt{-t}^n$ factor which appears in $M_n(s,t)$. It corresponds to the small b behaviour of $\tilde{M}_n$ obtained from formula (1b) [provided $M_n(s,t)$ has a good behaviour at large $|t|$].

We may give a generalization of formulae (2)

$$\tilde{M}_n(s,b) \propto b^n f(s,b)$$

where f(s,b) gives the geometry of all helicity amplitudes. This relation -- we may call it b universality -- seems to be approximately verified in several cases where one could reach different helicity amplidues such as Δ production processes[5]. This property has already been proposed for πN charge excnange, and has something to do with nuclear physics[11].

2.3 Basic ideas of our systematics

From these geometrical properties, it is possible to understand the successes and difficulties of the models based on Regge singularities.

In some cases Regge pole exchanges fit with a simple geometry. This has been observed first for ρ exchange: the trajectory $\alpha_\rho(t)$ vanishes at $t \sim -0.6$ which is the first zero of $J_1(R\sqrt{-t})$, ($R \sim 1$ fermi). The signature factor $1 - e^{-i\pi\alpha_\rho(t)}$ gives a nonsense wrong signature zero at $\alpha_\rho(t) = 0$. It is thus expected that in the n = 1 amplitude, the ρ exchange corresponds to a peripheral (or "δ", or "ring") geometry. Indeed such a geometry can be obtained only in the n = 1 amplitude [in the n = 0 amplitude, the standard ρ exchange would give rather a central (or "disk" or "Θ") geometry]. Now, what is observed is that the ρ contribution is peripheral[12] in both amplitudes (in the n = 1, because it has been said that a pure pole amplitude works, and in n = 0, because a peripheral zero -- the cross-over one -- is

actually observed). One can now understand the basis of our approach. We would say that it is not the Regge phase or zeros which are universal, but rather the geometry (b universality). We would say furthermore that the Regge pole phase is present in that amplitude for which it describes the universal geometry. As we will show later, this statement leads to simple systematics. Such a statement differs from the so-called dual absorption models[12] because it is valid for the whole amplitude (imaginary and real parts) and can be applied whatever the geometry is.

Since this question is in discussion about even signature exchanges[13], we have to understand how our approach can be applied to them (the qualitative reasoning which we have done on the ρ exchange works as well on vector exchanges like ω and K^* exchanges). Our present knowledge about even signature exchanges is less precise than that about odd signature exchanges (the cross-section for the $\pi^- p \to \eta n$ reaction which is the prototype reaction to study A_2 exchange is ten times smaller than the one of $\pi^- p \to \pi^0 n$, the P' or f_0 exchange is always mixed up with the Pomeron exchange, etc.). We are thus obliged to make more assumptions to extend eventual systematics to tensor exchanges. The key argument concerns exchange degeneracy and its breaking. It has been observed[13] that exchange degeneracy is essentially valid at the periphery (large b), whereas it is strongly violated in the centre (small b). Such a situation can be understood in terms of simple physical arguments. With Regge poles satisfying exchange degeneracy, it is normal that the large b region, associated with light particle exchanges, satisfies it. On the contrary, in the small b region associated with heavy exchanges including Regge cuts, one expects strong exchange degeneracy to fail, as in a dual scheme for Regge cuts[1]. Thus our conjecture is that exchange degeneracy is violated by the difference of the two geometries corresponding to vector and tensor exchange: if we assignate the δ geometry to vector exchanges, we are led to assignate the Θ geometry to tensor exchanges. But we have to check that they coincide at large b, owing to exchange degeneracy.

Such a prescription preserving the Regge phase for tensor exchange in one helicity amplitude can be obtained by assuming the "no compensation mechanism" for A_2, P', and K^{**} exchanges in the n = 0 amplitude, that is with a zero at $\alpha = 0$ corresponding to the J_1 zero in Eq. (2b). Actually this conjecture is supported by some phenomenological analysis[14]. The results we have obtained and which will be displayed below, give another piece of support.

2.4 Formulation of "Reggeometry"

We are now able to formulate the rules of our systematics.

2.4.1 "b universality"

For a given reaction, with well-defined t-channel quantum numbers, we assume b universality, that is

$$\tilde{M}_n(s,b) = g_n(s)\, b^n\, f(s,b) \qquad (3)$$

where $g_n(s)$ is a normalization function independent of b, b^n the kinematical factor, and f(s,b) a universal, independent of n, profile function.

This assumption is very constraining since, at a given energy, it reduces the arbitrariness to one complex amplitude and to normalization constants. We first note that since we allow the functions $g_n(s)$ to depend on s, they can be complex. It is also interesting to show how b universality allows the relation of two helicity amplitudes with different n. From (3) and the derivative relations between Bessel functions, one derives easily

$$M_{n'}(s,t) = \lambda_{n',n}(s)\,\sqrt{-t}^{\,n'}\left[\frac{d}{\sqrt{-t}\,d\sqrt{-t}}\right]^{n'-n}\left\{\frac{M_n(s,t)}{\sqrt{-t}^{\,n}}\right\} \qquad (4)$$

where $\lambda_{n',n}(s)$ is a complex function depending only on s.

Equation (4) would be very useful if one only wants to test b universality. For instance in the case of a $0 + \frac{1}{2} \to 0 + \frac{1}{2}$ reaction, like $\pi p \to \pi^0 n$, $M_1 = \lambda(s)\sqrt{-t}\, dM_0/dt$. An amplitude analysis could thus be done, just knowing the differential cross-section and the polarization, by solving differential equations.

2.4.2 Existence of a pure Regge pole amplitude

For any reaction with well-defined t-channel quantum numbers, we assume that there exists one helicity amplitude M_{n_P} which is described by a pure Regge pole exchange. For this amplitude we assume, up to adequate modifications for baryon exchanges, the following parametrization:

$$M_{n_R}(s,t) = \sqrt{-t}^{\,n_R}\left(\frac{s}{s_0}\right)^{\alpha(t)} i^{\frac{1+\xi}{2}}\left(1 - e^{-i\pi\alpha(t)}\right) \qquad (5)$$

where $\alpha(t)$ (or $\alpha + \frac{1}{2}$) is the trajectory and $\xi = (-)^J$ [or $\xi = (-)^{J+\frac{1}{2}}$] the signature of the meson (or baryon) exchange*). In this equation we see the nonsense wrong signature zero at $\alpha = 0$ for $\xi = -1$, and the no compensation mechanism zero at $\alpha = 0$ for $\xi = +1$.

2.4.3 Determination of n_R

The pure Regge pole behaviour is attributed to that amplitude for which the first nonsense zero is compatible with the chosen geometry. We thus constrain the trajectory to take their first nonsense value at a value of t corresponding to the first zero of a Bessel function of argument $R\sqrt{-t'}$, R = 1 fermi. This constraint can easily be satisfied for all trajectories satisfying exchange degeneracy, approximately linear and extrapolating known particles and resonances. The trajectories of ρ, A_2, ω, P', K^*, K^{**}, can coincide at zero and $t \sim -0.6$ (first zero of J_1). The N_α trajectory goes to $\alpha + \frac{1}{2} = 0$ at $u' \sim -0.2$ (first zero of J_0) and the Δ_δ trajectory to $\alpha + \frac{1}{2} = 0$ at $u' \sim -0.6$ (first zero of J_1).

According to our conjecture about violation of exchange degeneracy through the difference of geometries, we can now decide the value of n_R for each exchange. We assume the peripheral geometry if the first nonsense zero is at a wrong signature position ($\rho, \omega, K^*, N_\alpha$), and the central geometry in the other cases ($P', A_2, K^{**}, N_\gamma, \Delta_\delta$). From Eqs. (2a), (2b), and the nonsense values of the trajectories, we deduce the values of n_R for each Regge pole. The properties of the trajectories, the value of n_R, and the shape of the Regge pole amplitudes are displayed in Table 2.

2.4.4 Form of the non-Regge pole amplitudes

Equation (4) allows the computing of all the helicity amplitudes with $n \neq n_R$. Assuming linear trajectories, the derivations and integrations can be performed analytically. Before showing the results, we discuss briefly the energy behaviour of the functions $g_n(s)$. All the functions which appear in Table 1 are exponential in t with $\log s/s_o$ or $\log s/s_o - i\pi$ slopes. Thus the behaviour of $M_n(s,t)$ will be of the type $|\log s/s_o|^{n-n_R} (s/s_o)^{\alpha(t)}$. If we want all amplitudes to be dominated by a Regge pole term (plus eventually Regge cut terms), we are led to give $g_n(s)$ a behaviour of the type $|\log s|^{n_R-n}$. If furthermore we want to keep the correct signature properties (symmetry or antisymmetry on the change $s \to -s$), we have to symmetrize $\log s$, that is, to use $\frac{1}{2}[\log(s) + \log(-s)] = \log s - i\pi/2$. Thus all helicity amplitudes are written as:

---

*) Note that for baryon exchange, we use $\xi = (-)^{J+\frac{1}{2}}$, instead of the usual definition $(-)^{J-\frac{1}{2}}$.

$$M_n^{\rho,\omega,K^*}(s,t) = \lambda_n R_{n,1}(s,t',\alpha) \tag{6a}$$

$$M_n^{\rho',A_2,K^{**}}(s,t) = i\lambda_n R_{n,0}(s,t',\alpha) \tag{6b}$$

$$M_n^{N_\alpha}(s,t) = \lambda_n \sqrt{\frac{s_0}{s}}\, R_{n,0}(s,u',\bar{\alpha}) \tag{6c}$$

$$M_n^{\Delta_\delta}(s,t) = i\lambda_n \sqrt{\frac{s_0}{s}}\, R_{n,0}(s,u',\bar{\alpha}) \tag{6d}$$

where $\bar{\alpha} = \alpha + \frac{1}{2}$, λ_n are real constants and

$$R_{n,n_R}(s,t',\alpha) = \sqrt{-t'}^{\,n} \left(\text{Log}\, s/s_1 - i\pi/2\right)^{n_R-n} \left(\frac{s}{s_0}\right)^{\alpha(t)} \left\{ \left(\text{Log}\, s/s_0\right)^{n-n_R} - e^{-i\pi\alpha} \left(\text{Log}\, s/s_0 - i\pi\right)^{n-n_R} \right\} \tag{7}$$

From these formulae we can easily obtain the corresponding profile functions obviously exhibiting b universality

$$\tilde{M}_n^{\rho,\omega,K^*}(s,b) = \mu_n \tilde{R}_{n,1}(s,b,\alpha_0,\alpha') \tag{8a}$$

$$\tilde{M}_n^{\rho',A_2,K^{**}}(s,b) = i\mu_n \tilde{R}_{n,0}(s,b,\alpha_0,\alpha') \tag{8b}$$

$$\tilde{M}_n^{N_\alpha}(s,b) = \mu_n \sqrt{\frac{s_0}{s}}\, \tilde{R}_{n,0}(s,b,\bar{\alpha}_0,\alpha') \tag{8c}$$

$$\tilde{M}_n^{\Delta_\delta}(s,b) = i\mu_n \sqrt{\frac{s_0}{s}}\, \tilde{R}_{n,0}(s,b,\bar{\alpha}_0,\alpha') \tag{8d}$$

where α_0 and α' are intercept and slope of linear trajectories. ($\bar{\alpha}_0 = \alpha_0 + \frac{1}{2}$), μ_n are real constants, including powers of α' and $\tilde{R}_{n,n_R}$ are

$$\tilde{R}_{n,n_R}(s,b,\alpha_0,\alpha') = \frac{b^n}{2q^2} \left(\frac{s}{s_0}\right)^{\alpha_0-1} \left(\text{Log}\frac{s}{s_1} - i\frac{\pi}{2}\right)^{n_R-n} \left\{ \frac{e^{-b^2/4\alpha'\text{Log}\, s/s_0}}{\left(\text{Log}\, s/s_0\right)^{n_R+1}} - \frac{e^{-i\pi\alpha_0 - b^2/4\alpha'(\text{Log}\frac{s}{s_0} - i\pi)}}{\left(\text{Log}\, s/s_0 - i\pi\right)^{n_R+1}} \right\} \tag{9}$$

From formula (7) one can easily extract the complex zeros of the different amplitudes in the t-plane. The first zeros have to satisfy

$$\alpha(t_0) = i\,\frac{(n-n_R)}{\pi}\,\mathrm{Log}\left(\mathrm{Log}\,s/s_0 / \mathrm{Log}\,\frac{s}{s_0} - i\pi\right) \qquad (10)$$

In Fig. 1 we have drawn the complex zeros of ρ^0 and A_2^1, together with the signature ones of ρ^1 and A_2^0, in agreement with the expected geometrical zeros (see Table 1)

Note that these complex zeros of the full amplitude do not command exactly the zeros of real and imaginary parts, which depend also on the extra factors $[\log s/s_1 - i(\pi/2)]^{n_R-n}$: see formula (7). Nevertheless, they are related to the structures of the differential cross-sections and polarizations, provided they are not far from the real t-axis. This can give important direct tests of the proposed geometries.

3. APPLICATION TO MESON AND BARYON EXCHANGES

3.1 Parametrization

We want to apply our systematics to ρ, A_2, N_α, and Δ_δ exchanges in order to describe the following processes:

a) $\pi^- p \to \pi^0 n$: ρ

b) $\pi^- p \to \eta n$: $\frac{1}{\sqrt{3}} A_2$

c) $K^+ n \to K^0 p$: $\frac{1}{\sqrt{2}}(\rho + A_2)$

d) $K^- p \to \bar{K}^0 n$: $\frac{1}{\sqrt{2}}(\rho - A_2)$

e) $\pi^+ p \to p \pi^+$: $\frac{1}{3}(2N_\alpha + \Delta_\delta)$

f) $\pi^- p \to p \pi^-$: Δ_δ

g) $\pi^- p \to n \pi^0$: $\frac{\sqrt{2}}{3}(N_\alpha - \Delta_\delta)$

Each of these reactions is described by the two usual s-channel helicity amplitudes. For a given exchange, one amplitude only is of pure Regge form,

the remaining one being obtained, up to a kinematical factor and a coupling constant, by differentiating (for N_α, Δ_δ, and A_2) or integrating (ρ) the pure Regge amplitude with respect to the transfer variable. The corresponding analytical forms are given in Eqs. (6).

Apart from the well-known linear trajectories, the parameters to be determined are only four for each Regge exchange: two coupling constants λ_o^R and λ_1^R, and two scale parameters s_o^R and s_1^R, the role of which will be discussed later. Moreover, K-induced reactions (c) and (d) are related to (a) and (b) by imposing exact SU(3) symmetry. This permits expressing directly the amplitudes of reactions (c) and (d) in terms of the parameters of (a) and (b). [Results for η production take into account the branching ratio $\Gamma(\eta \to 2\gamma)/\Gamma(\eta \to \text{all modes})$ which is known to be 0.38.]

Results of our fit are summarized in Figs. (2) to (15). Our calculations have been performed without any minimization procedure. In fact, a given differential cross-section at one energy allows the calculation of parameters λ_o^R, λ_1^R, and s_o^R of the corresponding exchange. For instance, the shape of $d\sigma/dt(\pi^- p \to \pi^o n)$ at, say, $p_{lab} = 6$ GeV/c, determines λ_o^ρ, λ_1^ρ, and s_o^ρ: the flip amplitude being dominant λ_1^ρ, is fixed; then the forward point gives easily λ_o^ρ. As one interesting feature of the model, the parameter s_o^ρ is strongly constrained. It must give the form of the differential cross-section, but also fixes, once λ_o^ρ is known, the depth of the dip.

An analogue situation is encountered for the nucleon exchange and the corresponding differential cross-section:

$$\frac{d\sigma_N}{du} = \frac{1}{2}\left(3\left(\frac{d\sigma}{du}(\pi^+ p \to p\pi^+) + \frac{d\sigma}{du}(\pi^- p \to n\pi^o)\right) - \frac{d\sigma}{du}(\pi^- p \to p\pi^-)\right) \qquad \text{(cf. Fig. 14)}$$

the A_2 exchange and $d\sigma/dt(\pi^- p \to \eta n)$ (cf. Fig. 3), the Δ_δ exchange and $d\sigma/du(\pi^- p \to p\pi^-)$ (cf. Fig. 9). For these two last contributions, the strength of the flip amplitude is fixed at the right signature zero of the non-flip amplitude near $|t - t_{min}| \sim 0.6$.

This now leaves us mainly to determine the scale factor s_1^R from one polarization at a given energy for each exchange. In fact, the sensibility of polarizations to this parameter is easily explained by the fact that,

apart from the energy dependence, it induces a constant phase shift between the two s-channel amplitudes of the concerned exchange.

Proceeding along these lines, we have obtained the values of our 16 parameters as shown in Table 3. The resulting ρ, A_2, N_α, and Δ_δ amplitudes are shown at a given energy (p_{lab} = 6 GeV/c) on Figs. 16-19. We also give their impact parameter profiles (Figs. 20-23).

3.2 Results and discussions

From an inspection of our results, we can infer the following:

i) Essential features of data can be seen to be both qualitatively and quantitatively reproduced. The fit seems very satisfactory, in particular with regard to the small number of parameters and the energy range considered. We must emphasize how well the ρ exchange is described both in s and t.

ii) Note how excellently the strength and the shape of cross-sections and polarizations of the charge-exchange reactions $K^-p \to \bar{K}^0n$ and $K^+n \to K^0p$ are reproduced by our prediction. This indicates a remarkable agreement between SU(3) prediction and our parametrization.

iii) Backward elastic differential cross-sections and polarizations are adequately described at small transfer. However, some discrepancies appear for $|u| > 0.6$ $(GeV/c)^2$. For instance, the large values obtained for the $\pi^-p \to p\pi^-$ polarization (Fig. 11) disagree with the trend suggested by the data. Some aspects of the $\pi^+p \to p\pi^+$ polarization are not reproduced very well (Fig. 10).

The charge-exchange reaction is roughly described, but the fit is certainly less good than for elastic scattering.

iv) Our parametrization predicts a pronounced dip in the η production near $|t| = 1$ $(GeV/c)^2$. Such a structure is not clearly exhibited by the data, as can easily be seen at all incident momenta where measurements extend to large momentum transfers. In particular, the recent Serpukhov data at 40 GeV/c [15] contradict this prediction. But this dip is seen in the analogous case of $\pi^-p \to p\pi^-$ (cf. Fig. 9).

Let us now discuss more precisely the prominant features of our results and the corresponding structures of the amplitudes.

3.2.1 $\pi^- p \to \pi^o n$ polarization

It is well known from amplitude analysis[8] that a condition necessary to reproduce the correct shape of the polarization is that the real part of the non-flip amplitude must have no zero before the imaginary part. This typical feature is well given by our parametrization, as can be seen on Fig. 16.

We must outline that the factor $\log(s/s_1) - i(\pi/2)$, necessary to maintain asymptotic Regge behaviour and correct signature properties, also allows a particular satisfactory polarization at large t (cf. Fig. 4). This factor is equally essential to give the correct change of sign of polarizations given by A_2 and Δ_δ exchanges (cf. Figs. 5 and 11).

3.2.2 Line-reversal breaking and ρ-A_2 exchange degeneracy

It is well known that line reversal crossing symmetry between $K^- p \to \bar{K}^o n$ and $K^+ n \to K^o p$ is not verified below $p_{lab} = 6$ GeV/c where the exotic differential cross-section is larger in the very forward direction (cf. Fig. 6). This quite general feature of two-body line reversal reactions is obtained in our scheme, together with a natural mechanism of exchange degeneracy violation between ρ and A_2 exchanges: the geometry giving the shape of the amplitudes is different, as discussed in Section 2, although the trajectories are the same.

Furthermore, a comparison between ρ and A_2 amplitude profiles (cf. Fig. 21) shows that exchange degeneracy is approximately verified by our amplitudes at large b ($b > 1$ fermi). We then obtain phenomenologically this expected property of the amplitudes[11].

It is instructive to note that we predict that the "real" process will have a bigger cross-section than the "rotating" one, even at very high energies (cf. Fig. 6).

3.2.3 N_α-Δ_δ interference

The main drawback of all Regge models of backward scattering is the positive interference between N and Δ exchanges[16]. An amplitude analysis[17] shows that, in order to obtain this feature, the real part of the flip amplitude $M_o^{N\alpha}$ must possess a single zero near the signature point $|n| \sim 0.15$ (GeV/c)^2. By contrast, Regge models predict two nearby zeros.

Reggeometry provides us with a mechanism for this zero; it corresponds to the derivative of the double zero in the N_α non-flip amplitude (see Fig. 18) with a small shift given by the over-all factor $[\log s/s_1 - i(\pi/2)]$. In fact the interference thus obtained is not good enough to explain entirely the charge-exchange differential cross-section (cf. Fig. 12). Although the correct sign is obtained, the minimum is displaced by comparison to the experimental one (cf. Fig. 15).

3.3 Concluding remarks on the fit

Reggeometry works reasonably well for peripheral exchanges ρ and N_α. More detailed parametrization of the Regge input would probably improve the results. We can also easily guess that it will also work for other vector trajectories (such as K^* and ω).

The situation, though satisfactory, is not so clear for Δ_δ and A_2, and perhaps for P' and K^{**} exchanges. A comparison with the amplitude analysis of Ferro Fontan[17] shows that the main discrepancy with our Δ_δ parametrization comes from the real part of the non-flip amplitude (cf. Fig. 19). A similar defect seems to be shared by our A_2 amplitudes. Though our imaginary parts are not far from recent A_2 amplitude analysis[18] (double zero in the non-flip amplitude, single zero in the flip amplitude at the signature point), real parts are quite different. In particular, a double zero would be present in the real part of the non-flip amplitude and a single zero in the flip one. This is not in disagreement with b-universality, but does not correspond to the zero structure of a usual Reggeized amplitude. Is Reggeometry in question? Or does the choice of the tensor exchange geometry have to be revised? A separate test of these two independent assumptions would be necessary to discuss this problem in more detail

Finally, let us consider the energy dependence of our amplitudes. The dip in $\pi^- p \to \pi^0 n$ remains present at very high energies (cf. Fig. 2) in agreement with Serpukhov results[2]. Our parametrization gives an effective ρ trajectory in good agreement with experiment from 6 GeV/c to 48 GeV/c. Polarization is predicted not to change drastically with energy (cf. Fig. 4) in contradiction to some models[1].

4. DISCUSSION AND OUTLOOK

The results which have been displayed in the preceding section are rather encouraging. With a very simple and economical parametrization we have been able to reproduce the main features of the data and to propose

a solution to the puzzles which put difficulties to the current models (polarization in $\pi^- p \to \pi^0 n$, exchange degeneracy breaking in line reversed reactions, consistent description of meson and baryon exchanges).

Indeed there remain some discrepancies. We think that it is possible to overcome these difficulties without alterating the simplicity of the parametrization. Using curved trajectories should allow us to get rid of the difficulties at large t. In the backward region, we have not introduced any N_γ contribution. Now, there exist no reasons to claim that this contribution is strictly zero. Introducing it could permit the improvement of the interference between $I = \frac{1}{2}$ and $I = \frac{3}{2}$ contributions.

Another step consists in applying the systematics to many more reactions: in particular, high spin particle production reactions (vectors, tensors, nuclear isobars), in order to test the validity of the systematics for high n amplitudes. It is interesting to note that Reggeometry provides a natural mechanism to explain the filling of the dips when the number of helicity amplitudes involved in the reaction increases. For instance, this phenomena has been experimentally observed in backward production, whereas a pronounced dip occurs in the backward $\pi^+ p \to p\pi^+$ cross-section near $u \sim -0.15$ $(GeV/c)^2$, this minimum is no longer present in backward pion photoproduction[19] and perhaps in ρ and f^o production[20]. However, the same u-channel exchanges are allowed in the four reactions and the filling of the dip is hard to understand from a conventional Regge framework. On the other hand, since in the Reggeometry scheme one helicity amplitude only must possess this dip, the disappearance of such structures when the number of amplitudes increases is then expected.

The same kind of remarks can be made about the extrapolation in the mass, for high mass exclusive, inclusive and semi-inclusive reactions. In the multi-Regge formalism, the scale parameter s_o is, in a natural way, equal to the square of the produced mass. Thus in such reactions we would know the scale parameter. When the missing mass squared M^2 increases, one expects the produced spin to increase also as well as the number of helicity amplitudes. For instance, Reggeometry has been applied successfully to $\pi^+ p \to \pi^o (p\pi^+)$ and allows explaining the filling of the dips for high $(p\pi^+)$ mass and the relation between the slope of the cross-section and this missing mass[21].

Before going into the discussion of the more theoretical aspects of Reggeometry, we have to say a few words on the limitations and drawbacks.

The first limitation concerns the Pomeron. The behaviour of total cross-sections at high energy shows that the Pomeron is more complicated than a simple Regge pole. We do not know yet whether Reggeometry could apply to the Pomeron also. There exist some indications that the Pomeron contributions satisfy b-universality[22], but one does not know whether there exists any helicity amplitude which can be described by a pure pole exchange. Indeed we could extend our analyses to elastic and diffractive reactions by putting a standard phenomenological contribution to account for the Pomeron. More interesting could be to amplitude analyse the Pomeron contribution from elastic data and from a description based on Reggeometry for the non-Pomeron contributions.

The most severe limitation of Reggeometry concerns the t-channel singularities. In our parametrization, it can be remarked that we have omitted the particle poles in the t-channel. This ommission was useful for technical interest; in fact the existence of t-channel poles [factors like $\Gamma[1 - \alpha(t)]$, $1/\sin \pi\alpha(t)$ or $1/t - m^2$] complicates the calculations when one has to integrate with respect to t. Indeed the consequence of this ommission is not very important when the nearest pole in the t-channel is rather far from the physical region. Nevertheless, it is a drawback, since for instance we are not able to extrapolate our πN backward amplitude to the nucleon pole as there is no nucleon pole!

Actually the difficulty of taking poles into account is more than simply technical. One can easily be convinced that t-channel poles are incompatible with b-universality: a pole at $t = m^2$ gives profile functions which, at large b, behave like $e^{-mb}/\sqrt{b}$ for all n. So if one has a pole in the Regge amplitude ($n = n_R$), in all other amplitudes the b^n factor will alterate the behaviour at large b and thus change the nature of the singularity at $t = m^2$. This difficulty is particularly clear in the case of pion exchange, for which we know that the most striking features of the data are explained by the nearby pion physical pole. That is why we expect Reggeometry to fail in describing pion exchange.

In order to conclude we wish to list the theoretical teachings which one can draw from Reggeometry and its first applications.

1. The strongest statement on which this approach relies seems to be b-universality. This property, which is quite familiar in low-energy nuclear physics, is probably the key to a classical or semiclassical interpretation

of our approach. It is interesting to note that b-universality also underlies the s-channel approach of Schrempp and Schrempp[23] who have reached results quite similar to ours. We think that systematical tests of this assumption would be very interesting.

The incompatibility of t-channel poles and b-universality suggests a picture in which the "core" that is the region up to, say, 2 fermis satisfies essentially b-universality, whereas the large b-tail does not. A piece-wise approach of these two regions with a smooth connection between them could lead to an improved description.

2. The other empirical laws of Reggeometry, like the existence of two geometries, or the existence of one Regge pole-like amplitude, or the assignation of a geometry to a Regge exchange according to the signature at the first nonsense point, are more or less conjectural. Indeed, the coincidence of nonsense zeros and geometrical zeros is striking. But, whereas the derivation of the systematics was very natural for ρ, ω, K^* and N_α exchanges, its extension to tensor and Δ_δ exchanges is much more conjectural. The first results obtained are encouraging, but further careful studies are certainly needed.

3. It is straightforward to analyse our amplitudes in terms of t-channel Regge singularities. Expanding the amplitudes in power of 1/log s, one gets a pole + cut expansion (the cut contribution obviously vanishes for $n = n_R$). Comparison with the absorption models shows the following differences between the two types of cuts:

i) in our approach the branch point trajectory coincides with the pole trajectory, whereas the absorptive branch points lie on the AFS trajectories which are much flatter;

ii) the variation with respect to n of the strength of the cut contributions is completely different in the two approaches;

iii) the phase of the cuts are also different: in the $n = 0$ ρ amplitude, the cut we get absorbs the imaginary part and anti-absorbs the real part of the pole term; the absorptive cut absorbs both real and imaginary parts.

It is interesting to note that systematically the differences between the two types of cuts exist about features which, as we mentioned at the beginning, put severe difficulties for absorption models. Somehow the

results we have obtained allow us to spot the difficulties of standard Regge cut models. We think that Regge cuts exist and are important. We even think that the branch points lie on AFS trajectories (the discontinuities across the cuts would be very small near the branch point and would be rather concentrated near the associated Regge poles). We think that the whole Reggeon calculus (computation of Regge cuts) should be revised: evaluation of the cut discontinuities, in particular in the vicinity of the pole, of the strength and the phase of the cut contributions according to the helicity, should be re-examined.

Acknowledgements

We wish to thank A. Morel for having pointed out to us the open problems in backward scattering, and the colleagues of the Theoretical Study Division (CERN) for fruitful discussions.

Table 1

Order of Bessel function	First zero (R = 1 f)	Observed structure
n = 0	$t = -0.25\ GeV^2$	"cross-over zero" dip in $\pi^+ p \to p\pi^+$
n = 1	$t = -0.585\ GeV^2$	dip in $\pi^- p \to \pi^0 n$
n = 2	$t = -1.05\ GeV^2$	dip or shoulder in $\pi^- p \to \eta n$ and $\pi^- p \to p\pi^-$

Table 2

Exchange	ξ	1st signature zero (Wrong or Right)	Order n of J_n whose 1st zero is the 1st N.S. zero	Gecmetry	n_R	Regge pole amplitude $M_n(s,t)$
ρ, ω, K^*	-	$\alpha = 0$ W.S.	1	δ	1	$\sqrt{-t}\left(\frac{s}{s_0}\right)^{\alpha(t)}\left(1 - e^{-i\pi\alpha(t)}\right)$
P', A_2, K^{**}	+	$\alpha = 0$ R.S.	1	θ	0	$i\left(\frac{s}{s_0}\right)^{\alpha(t)}\left(1 - e^{-i\pi\alpha(t)}\right)$
N_α	-	$\bar{\alpha} = \alpha + \frac{1}{2} = 0$ W.S.	0	δ	0	$\left(\frac{s}{s_0}\right)^{\alpha(u)}\left(1 - e^{-i\pi\alpha(u)}\right)$
Δ_δ	+	$\bar{\alpha} = \alpha + \frac{1}{2} = 0$ R.S.	1	θ	0	$i\left(\frac{s}{s_0}\right)^{\alpha(u)}\left(1 - e^{-i\pi\bar{\alpha}(u)}\right)$

Table 3

Adjustable parameters and linear trajectories used in the fit

Exchanged trajectories	λ_o	λ_1	s_o	s_1	Trajectories
ρ	13.7	-39.0	0.32	0.32	0.5 + 0.9t
A_2	-18.2	+80.0	0.3	2.0	0.5 + 0.9t
N_α	-122.4	-55.0	0.85	0.2	-0.35 + u
Δ_δ	-5.4	-8.56	2.8	1.5	u

REFERENCES

1) G. Girardi, R. Lacaze and R. Peschanski, Nuclear Phys. B69, 107 (1974).

2) V.N. Bolotov et al., Nuclear Phys. B73, 365 (1974).

3) W.F. Baker et al., "Total cross-sections of $\pi^{\pm}$, $K^{\pm}$, p, and $\bar{p}$ on hydrogen and deuterium between 50 and 200 GeV/c" (preliminary FNAL results).

4) G.A. Ringland, "Models for non-diffractive two-body reactions", Aix Conference Reports, Suppl. au Journal de Physique 34, Fasc. 11-12, 292 (1973).

5) J.P. de Brion and R. Peschanski, CERN Preprint TH.1848 (1974) (to be published in Nuclear Phys. B).

6) M. Davier and H. Harari, Phys. Letters 35B, 239 (1971).

7) R. Diebold, "Recent spectrometer results on non-diffractive processes", Aix Conference Reports, Suppl. au Journal de Physique 34, Fasc. 11-12, 284 (1973).

8) R.L. Kelly, Phys. Letters 39B, 635 (1972).

9) V.N. Bolotov et al., Nuclear Phys. B73, 387 (1974).

10) D.P. Owen et al., Phys. Rev. 181, 1794 (1969).

11) H. Høgaasen, Physica Norvegica, Vol. 5, 219 (1971);
F. Halzen, Argonne National Laboratory Preprint, ANL/HEP (June 1974) (other references are quoted by the author).

12) H. Harari, Ann. of Phys. (NY) 63, 432 (1971).

13) P.R. Stevens, Riverside Preprint, UCR-73-5 (1973).

14) V. Barger and R.J.N. Phillips, Phys. Rev. 187, 2210 (1969);
H. Harari and Y. Zarmi, Phys. Rev. 187, 2230 (1969);
J.D. Jackson, Lund Conference Reports (1969);
R. Johnson and F. Elevkjaer, CERN Preprint TH.1899 (1974).

15) W.D. Apel et a., "A study of the reaction $\pi^- p \to \pi n$ at momenta up to 40 GeV/c, paper submitted to the London Conference, July 1974.

16) F. Hayot and A. Morel, Phys. Rev. D8, 223 (1973);
V. Barger and M.G. Olsson, Phys. Rev. D5, 2736 (1972).

17) C. Ferro Fontan, CERN Preprint TH.1490 (1972) (unpublished).

18) G. Girardi, C. Godreche and H. Navelet, Saclay Preprint DPH-T/74-10 (1974).

19) R.L. Anderson et al., Phys. Rev. Letters 23, 721 (1969).

20) S. Dado et al., Phys. Letters B50, 275 (1974).

21) J.P. Ader, S. Humble, R. Lacaze and R. Peschanski (in preparation).

22) S. Humble, CERN Preprint TH.1827 (1974).

23) B. Schrempp and F. Schrempp, CERN Preprint TH.1812 (1974) (to be published in Nuclear Phys. B).

24) A.V. Stirling et al., Phys. Rev. Letters 14, 763 (1965);
P. Sonderegger et al., Phys. Letters 20, 75 (1966);
M. Yvert, private communication (1968);
M.A. Wahlig, Phys. Rev. 168, 1515 (1968).

25) O. Guisan et al., Phys. Letters 18, 200 (1963).

26) $\pi^- p \to \pi^0 n$ and $\pi^- p \to \eta n$ at p_{lab} = 5, 8 GeV/c:
P. Bonamy et al., Nuclear Phys. B52, 392 (1973);
$\pi^- p \to \pi^0 n$ at 5 GeV/c:
D. Hill et al., Phys. Rev. Letters 30, 239 (1973).

27) P. Astbury et al., Phys. Letters 23, 396 (1966);
D. Cline, J. Penn and D.D. Reeder, Nuclear Phys. B22, 247 (1970);
A. Firestone et al., Phys. Rev. Letters 25, 958 (1970).

28) W. Beusch et al., Phys. Letters B46, 744 (1973).

29) H. Aoi et al., Phys. Letters 35B, 90 (1973).
H. Aoi et al., report unpublished.

30) J.P. Boright et al., Phys. Rev. Letters 24, 964 (1970); Phys. Letters 33B, 615 (1970).

FIGURE CAPTIONS

Fig. 1 : Complex zeros of ρ and A_2 "Reggeometric" amplitudes: variation with the energy.

Fig. 2 : Charge-exchange differential cross-sections for p_{lab} varying from 6 GeV/c to 48 GeV/c [data from Refs. 2) and 24)].

Fig. 3 : Differential cross-sections for $\pi^- p \to \eta n$ from p_{lab} = 6 GeV/c up to p_{lab} = 48 GeV/c [data taken from Refs. 9), 13), and 25)].

Fig. 4 : Polarizations for $\pi^- p \to \pi^o n$ at 5 GeV/c and 8 GeV/c [Ref. 26)] with our prediction at 40 GeV/c.

Fig. 5 : Polarization for $\pi^- p \to \eta n$ at 5 GeV/c and 8 GeV/c [Ref. 26)] with our prediction at 40 GeV/c.

Fig. 6 : Differential cross-sections for $K^- p \to \bar{K}^o n$ and $K^+ n \to K^o p$ at 6 and 12 GeV/c [data from Ref. 27)] with our predictions at 40 GeV/c and with a comparison of the two reactions (dashed lines for $K^+ n \to K^o p$ in the $K^- p \to \bar{K}^o n$ results).

Fig. 7 : Polarizations for $K^- p \to \bar{K}^o n$ [Ref. 28)] and $K^+ n \to K^o p$ at p_{lab} = 8 GeV/c with our predictions at 40 GeV/c.

Fig. 8 : $d\sigma/du$ for $\pi^+ p \to p\pi^+$ at 5.9 GeV/c and 9.85 GeV/c [data from Ref. 9)] and our prediction at 40 GeV/c.

Fig. 9 : $d\sigma/du$ for $\pi^- p \to p\pi^-$ at 5.9 GeV/c and 9.85 GeV/c [data from Ref. 10)] and our predictions at 40 GeV/c.

Fig. 10 : Polarization for $\pi^+ p \to p\pi^+$ at 5.9 GeV/c [data from Ref. 29)] (the dashed line gives a solution with a smaller scale factor $s_1^{N_\alpha} \simeq 0.001$).

Fig. 11 : Polarization for $\pi^- p \to p\pi^-$ at 6 GeV/c [data from Ref. 29)].

Fig. 12 : $d\sigma/du$ for $\pi^- p \to n\pi^o$ at 5.9 GeV/c and 10.1 GeV/c and predicted curve at 40 GeV/c [data from Ref. 30)].

Fig. 13 : Predicted charge-exchange polarization in the backward direction at p_{lab} = 6 GeV/c.

Fig. 14 : The modulus squared of the isospin $\frac{1}{2}$ amplitude σ_N at 5.9 GeV/c [data quoted in Ref. 16)].

Fig. 15 : N_α, Δ_δ interference at 5.9 GeV/c [data quoted in Ref. 16)].

Fig. 16 : The t-dependence of our amplitudes for $\pi^- p \to \pi^o n$ (ρ exchange) at p_{lab} = 6 GeV/c. Solid (dashed) curves for real (imaginary) parts.

Fig. 17 : The t-dependence of our amplitudes for $\pi^- p \to \eta n$ (A_2 exchange) and p_{lab} = 6 GeV/c. Solid (dashed) curves for real (imaginary) part.

Fig. 18 : N_α s-channel helicity amplitudes evaluated at 6 GeV/c. Solid (dashed) curves for real (imaginary) parts.

Fig. 19 : Δ_δ s-channel helicity amplitudes evaluated at 6 GeV/c. Solid (dashed) curves represent real (imaginary) parts. The solid points represent Re M_o^Δ obtained by Ferro Fontan[17].

Fig. 20 : Hankel transform of ρ amplitudes in arbitrary units versus the impact parameter in fm. The solid (dashed) lines represent the real (imaginary) parts.

Fig. 21 : Hankel transform of A_2 amplitudes versus the impact parameter in fm. The solid (dashed) lines represent the real (imaginary) parts. The solid points are the imaginary parts of ρ amplitudes.

Fig. 22 : Hankel transform of N_α amplitudes. Solid (dashed) lines represent real (imaginary) parts.

Fig. 23 : Same as Fig. 22, but for Δ_δ amplitudes.

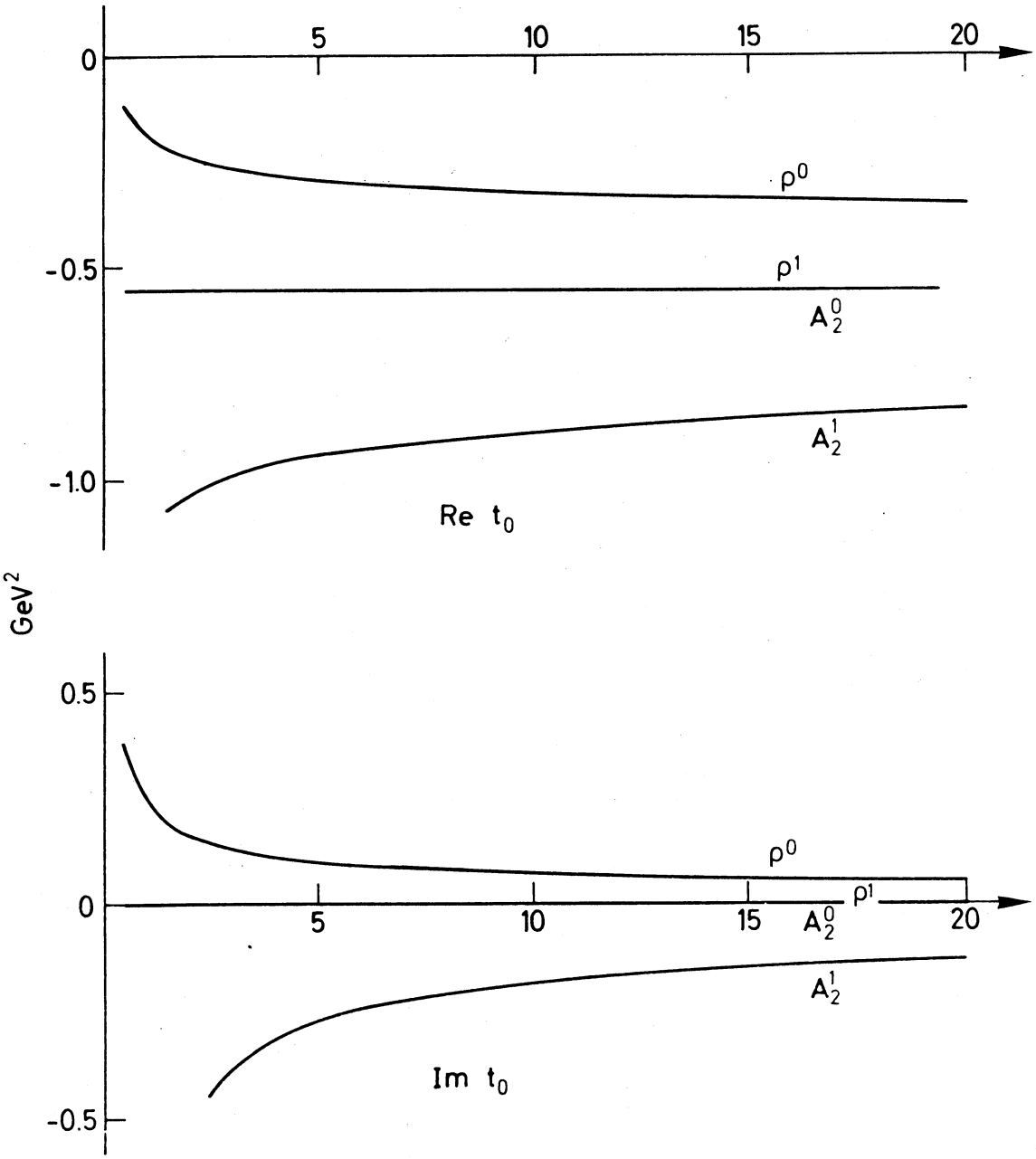

Fig. 1

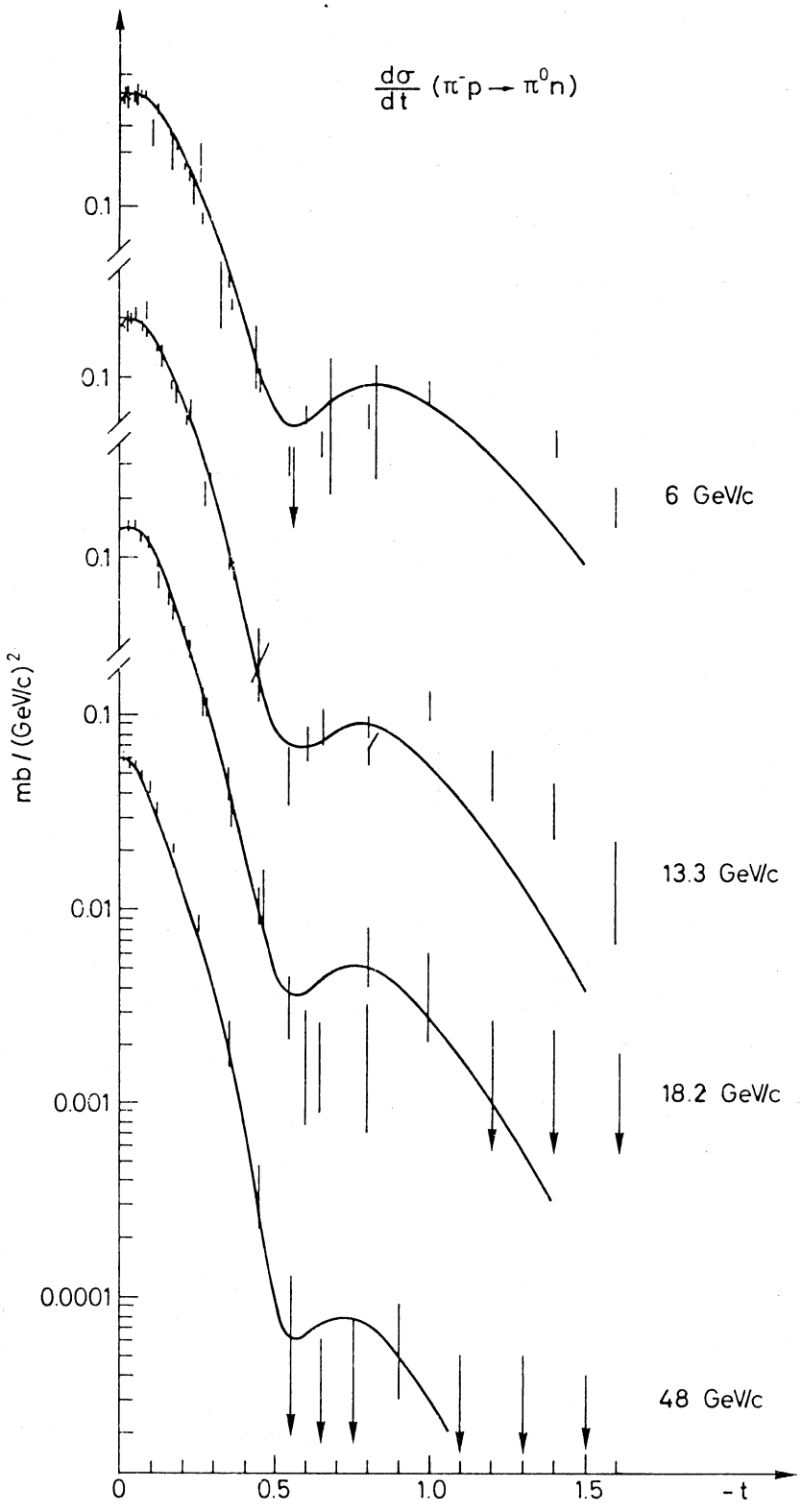
$\frac{d\sigma}{dt}$ ($\pi^- p \to \pi^0 n$)
mb / (GeV/c)^2
0.1
0.1
0.1
0.01
0.001
0.0001
6 GeV/c
13.3 GeV/c
18.2 GeV/c
48 GeV/c
0
0.5
1.0
1.5
- t

Fig. 2

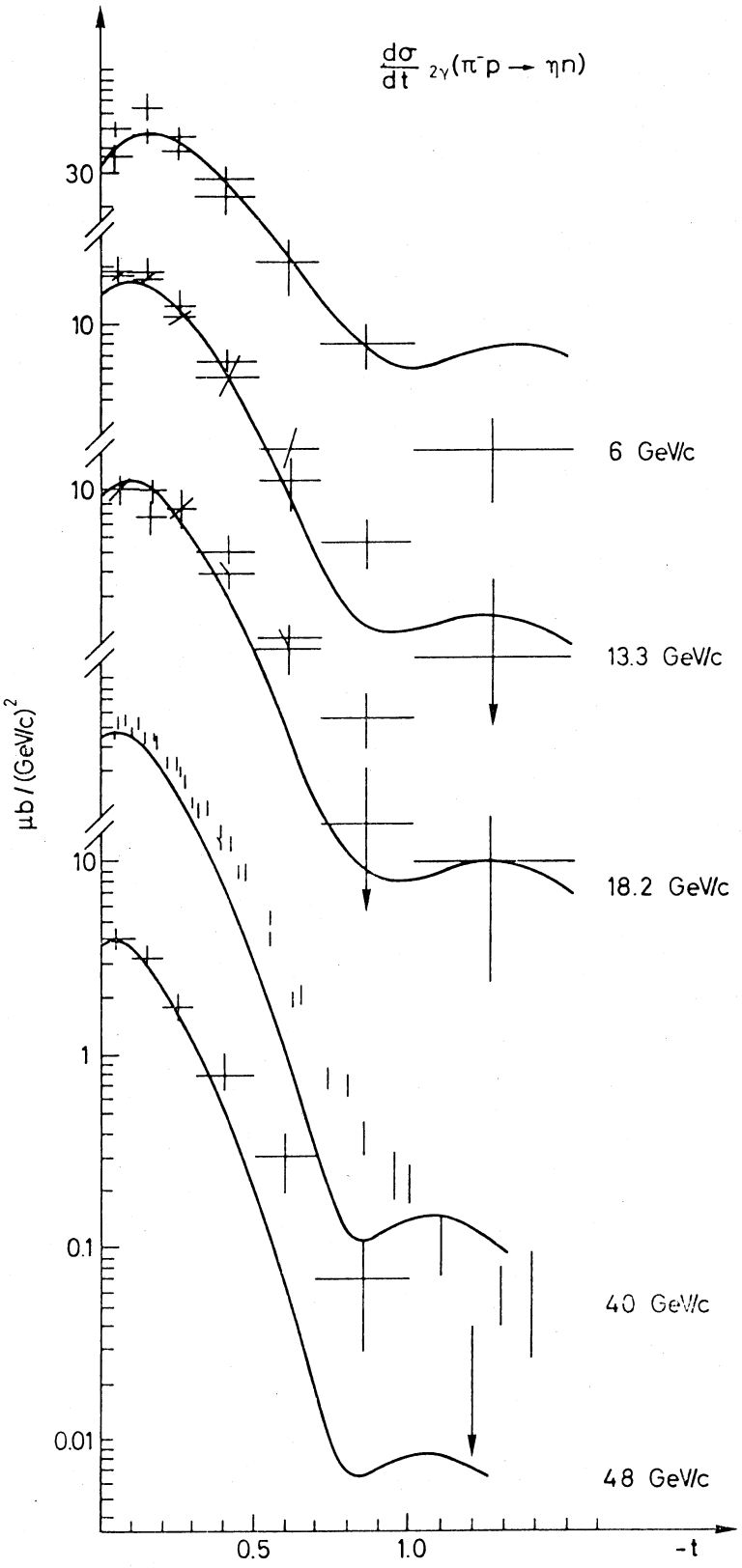
$\frac{d\sigma}{dt}_{2\gamma}(\pi^- p \to \eta n)$
30
10
10
10
1
0.1
0.01
μb / (GeV/c)²
6 GeV/c
13.3 GeV/c
18.2 GeV/c
40 GeV/c
48 GeV/c
0.5
1.0
-t

Fig. 3

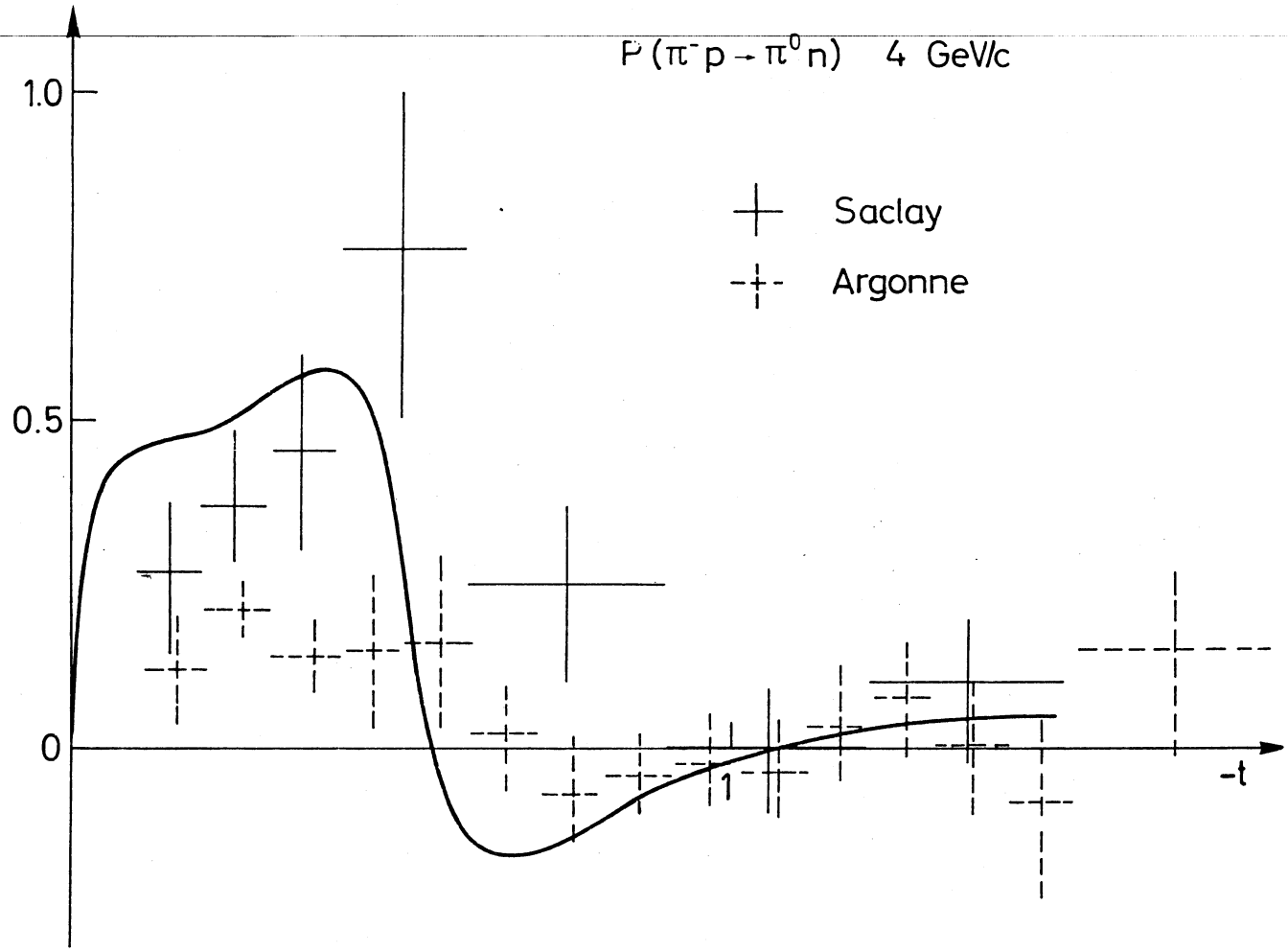
P (π⁻p → π⁰n) 4 GeV/c
1.0
0.5
0
Saclay
Argonne
1
-t

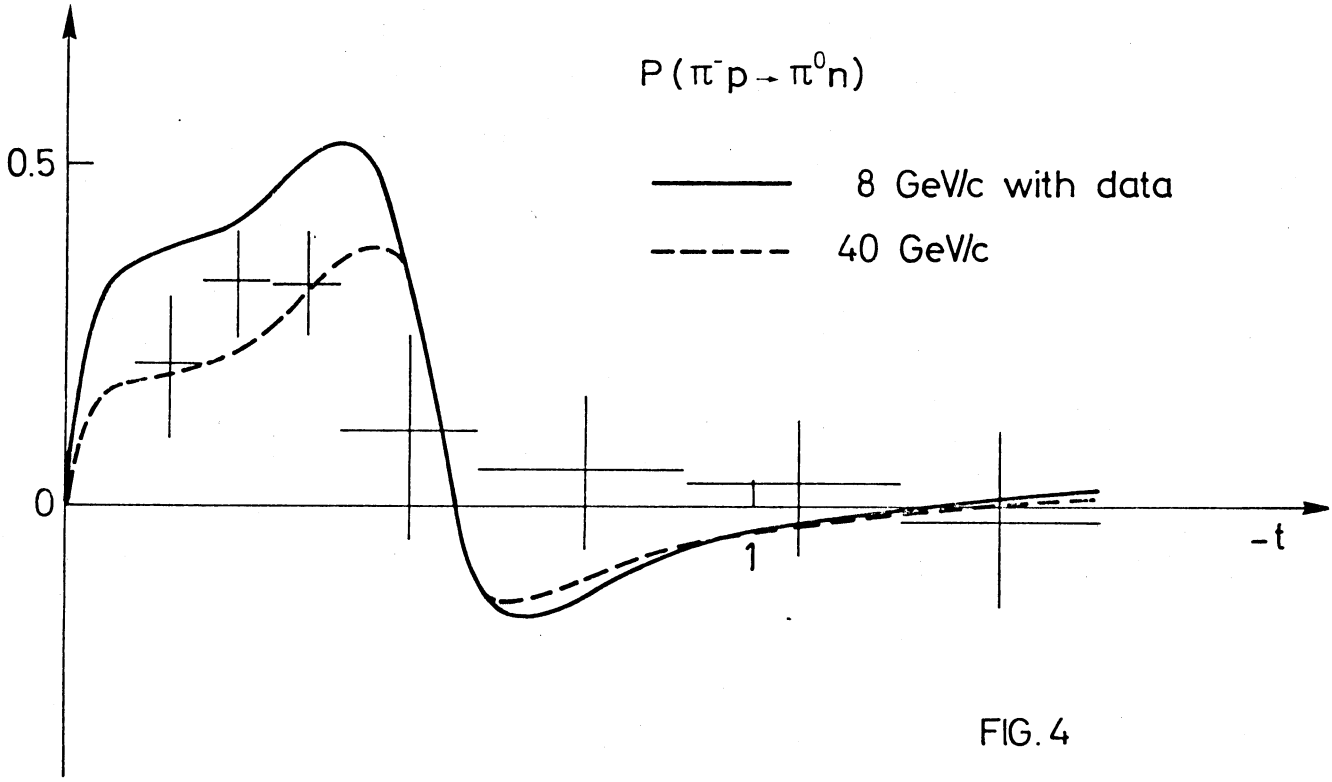
P (π⁻p → π⁰n)
0.5
0
8 GeV/c with data
40 GeV/c
1
-t

FIG. 4

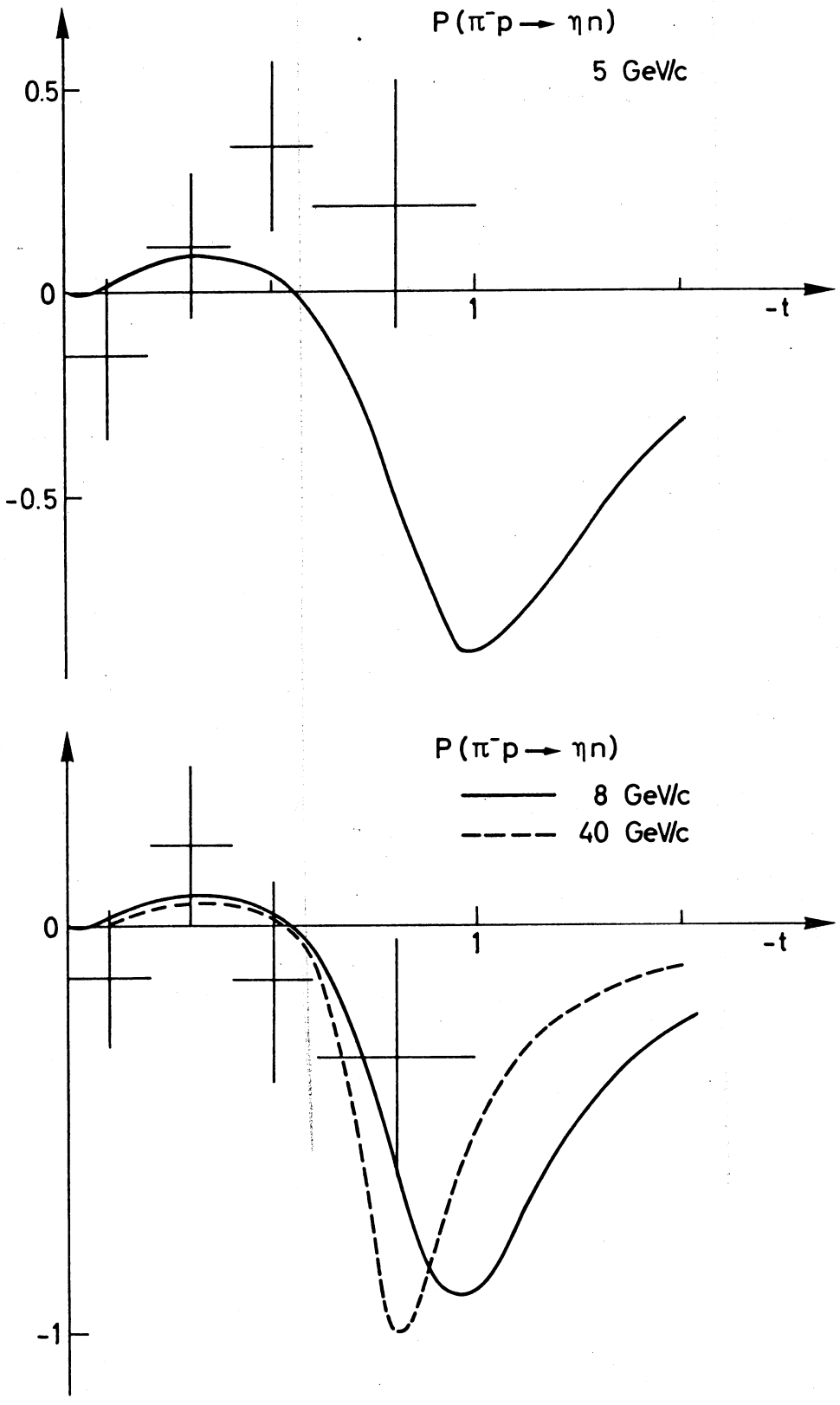

Fig. 5

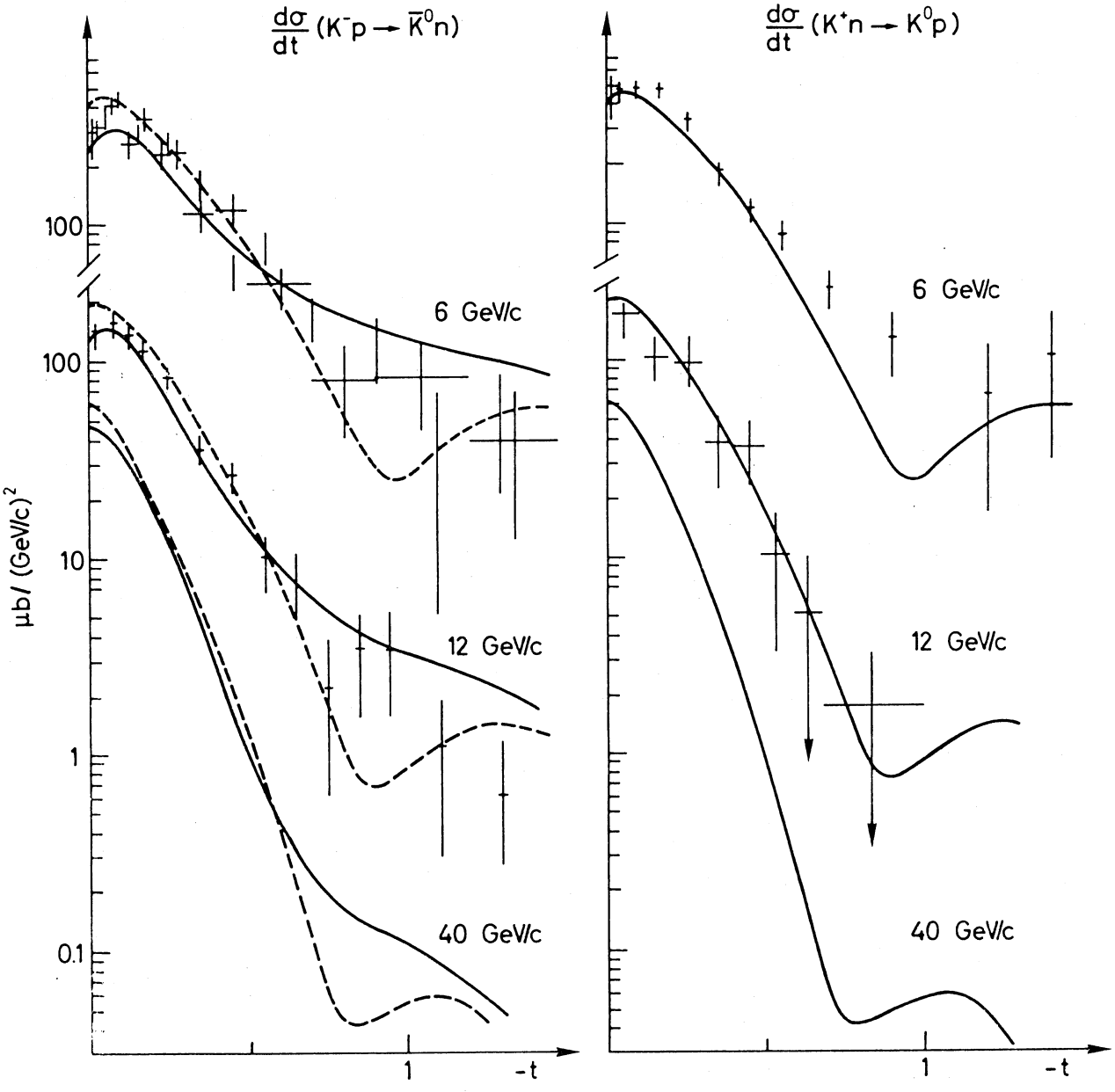
dσ/dt (K⁻p → K̄⁰n)
dσ/dt (K⁺n → K⁰p)
μb/ (GeV/c)²
100
10
1
0.1
6 GeV/c
12 GeV/c
40 GeV/c
1
-t

Fig. 6

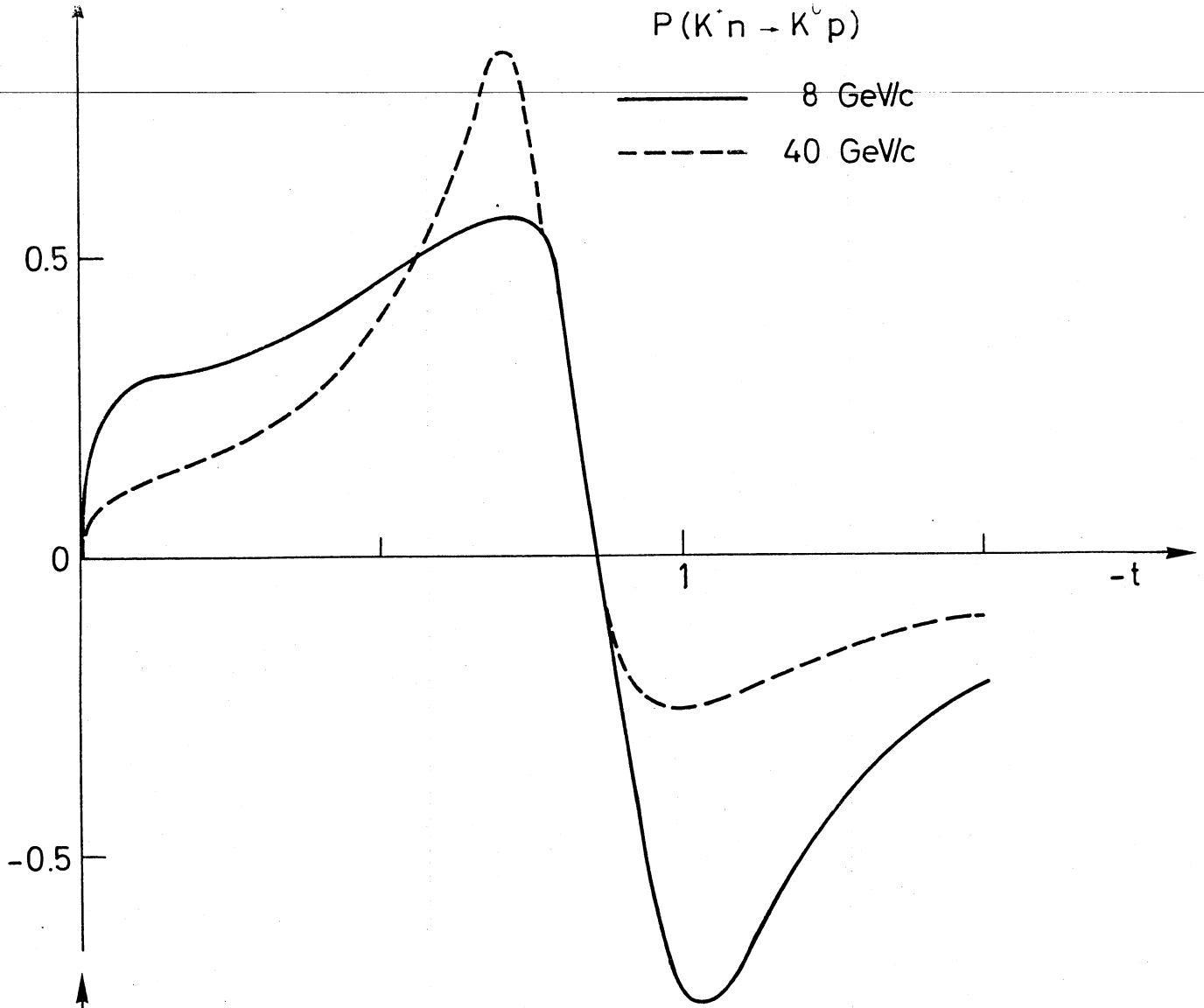
P(K⁻n → K⁰p)
8 GeV/c
40 GeV/c
0.5
0
-0.5
1
-t

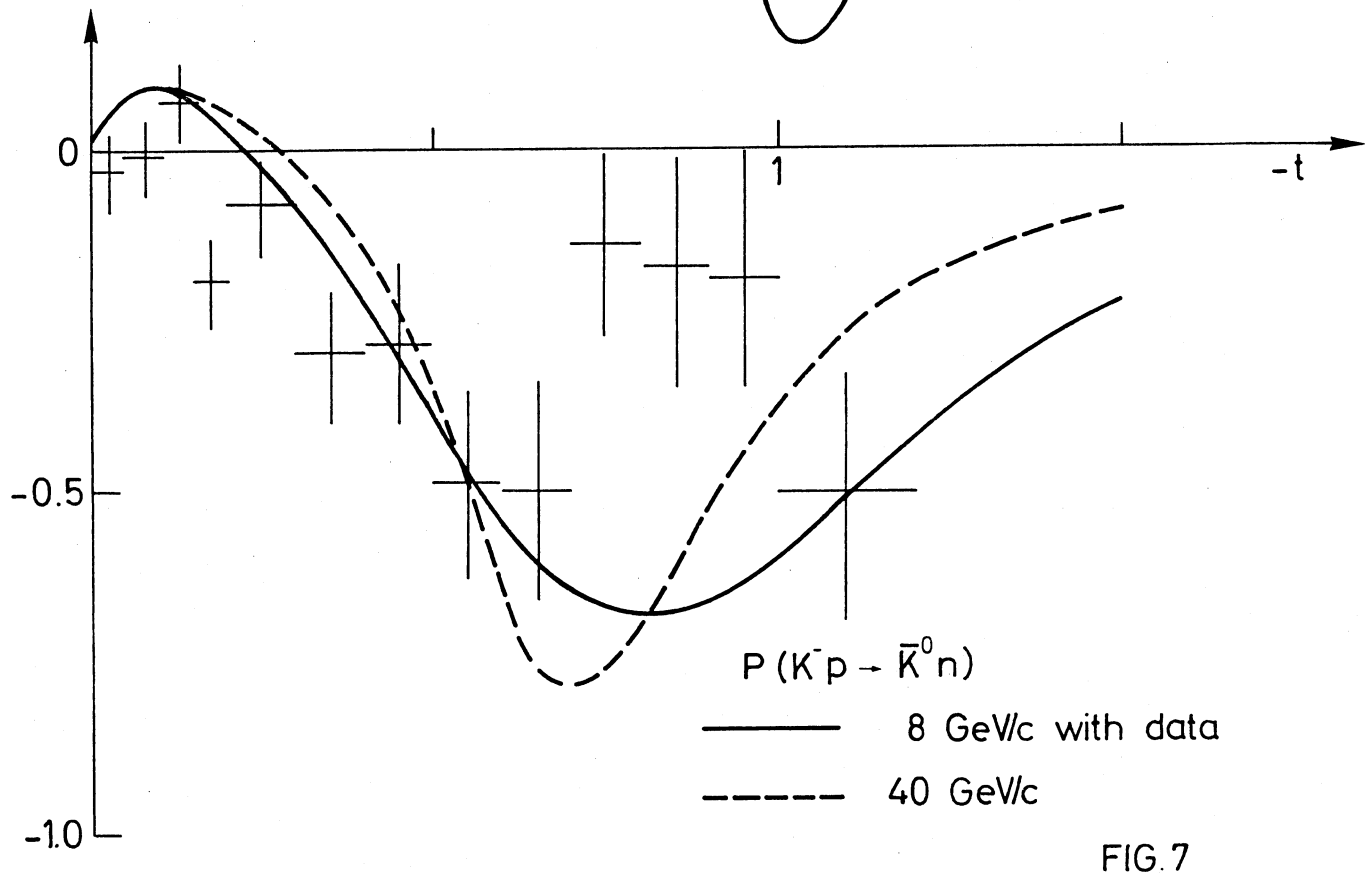
0
-0.5
-1.0
1
-t
P(K⁻p → K̄⁰n)
8 GeV/c with data
40 GeV/c

FIG. 7

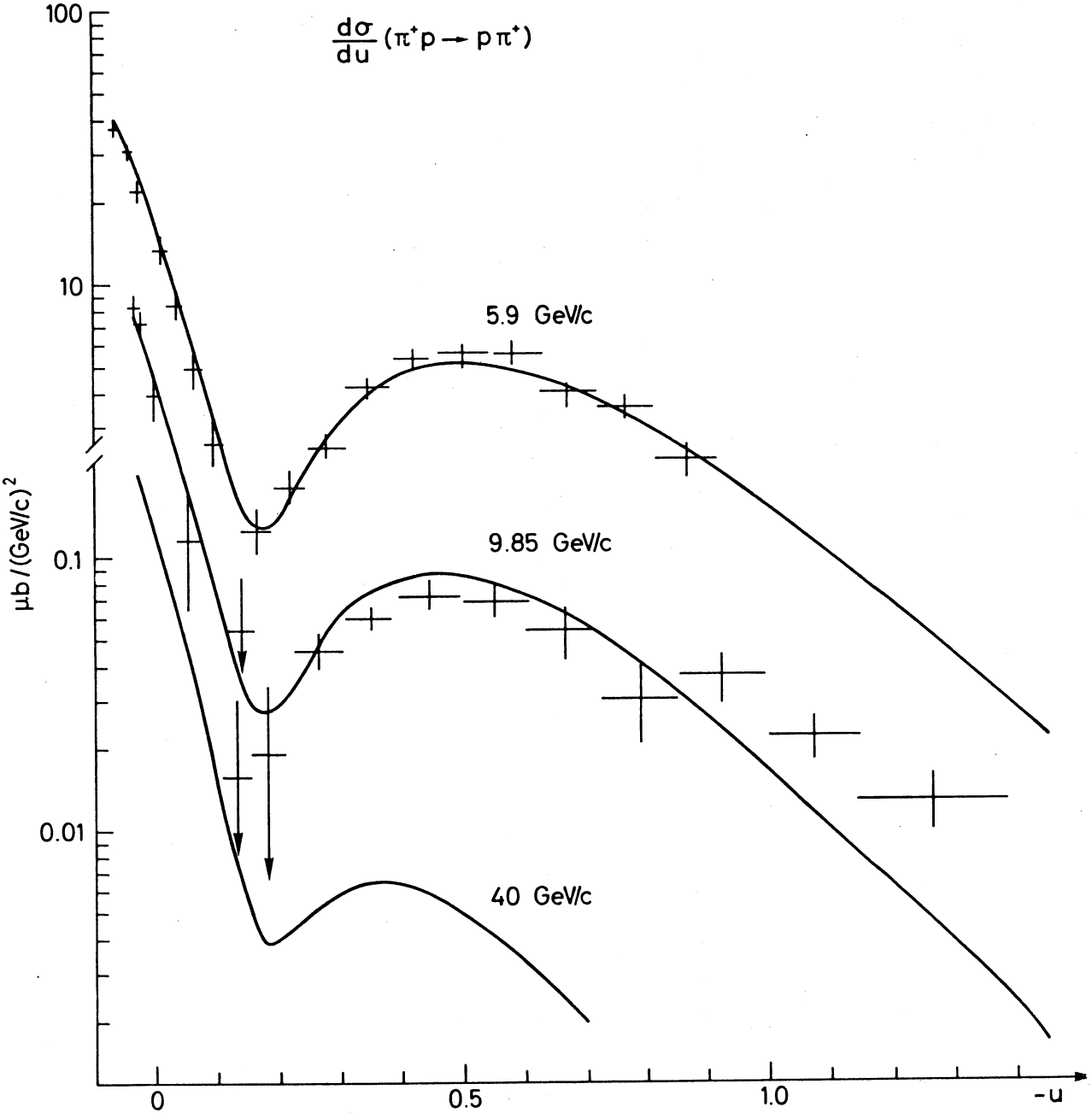
100
10
0.1
0.01
$\frac{d\sigma}{du}(\pi^+p \to p\pi^+)$
μb/(GeV/c)²
5.9 GeV/c
9.85 GeV/c
40 GeV/c
0
0.5
1.0
-u

Fig. 8

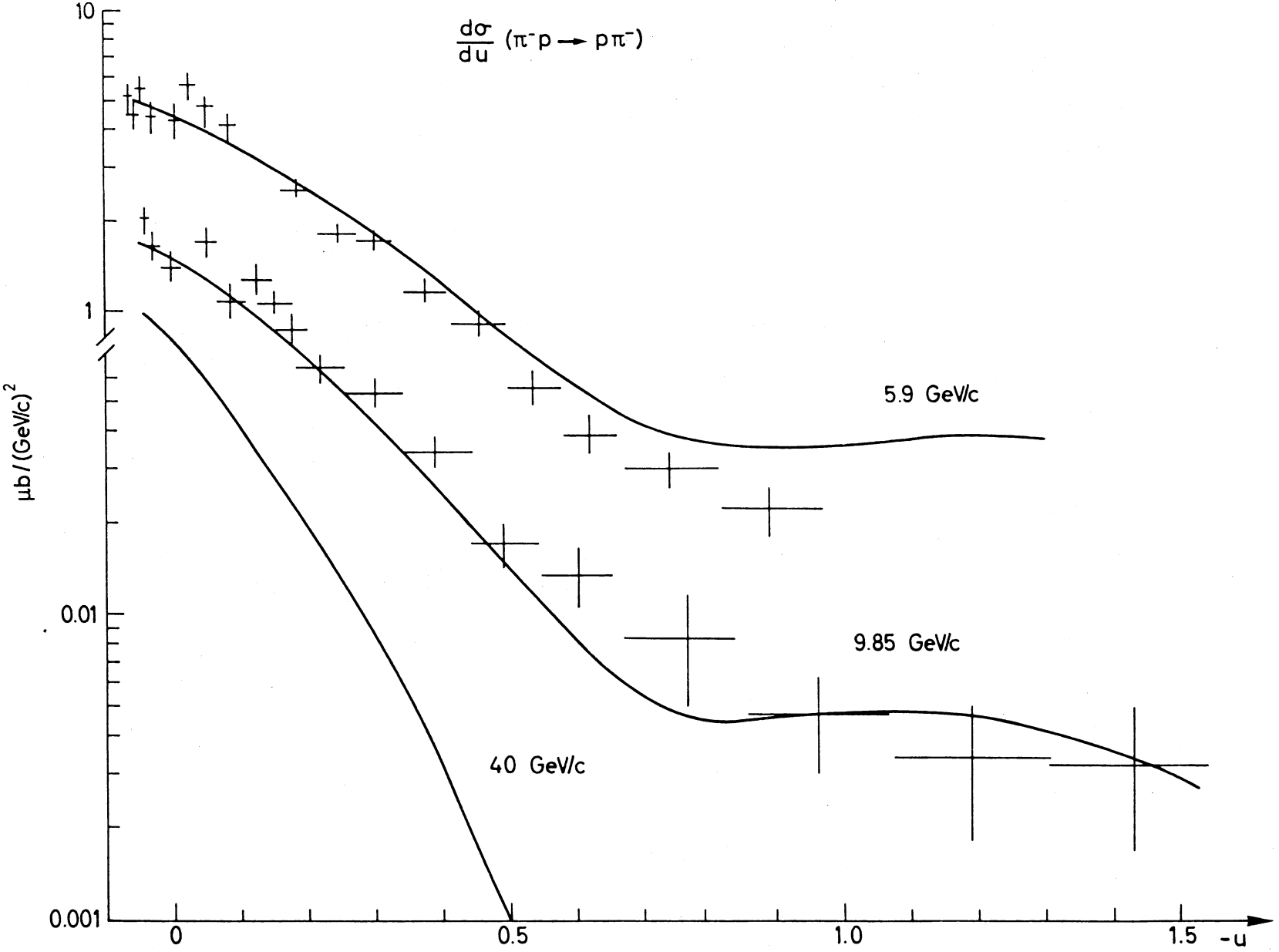
$\frac{d\sigma}{du}$ ($\pi^- p \rightarrow p\pi^-$)
10
1
0.01
0.001
μb / (GeV/c)^2
5.9 GeV/c
9.85 GeV/c
40 GeV/c
0
0.5
1.0
1.5
-u

Fig. 9

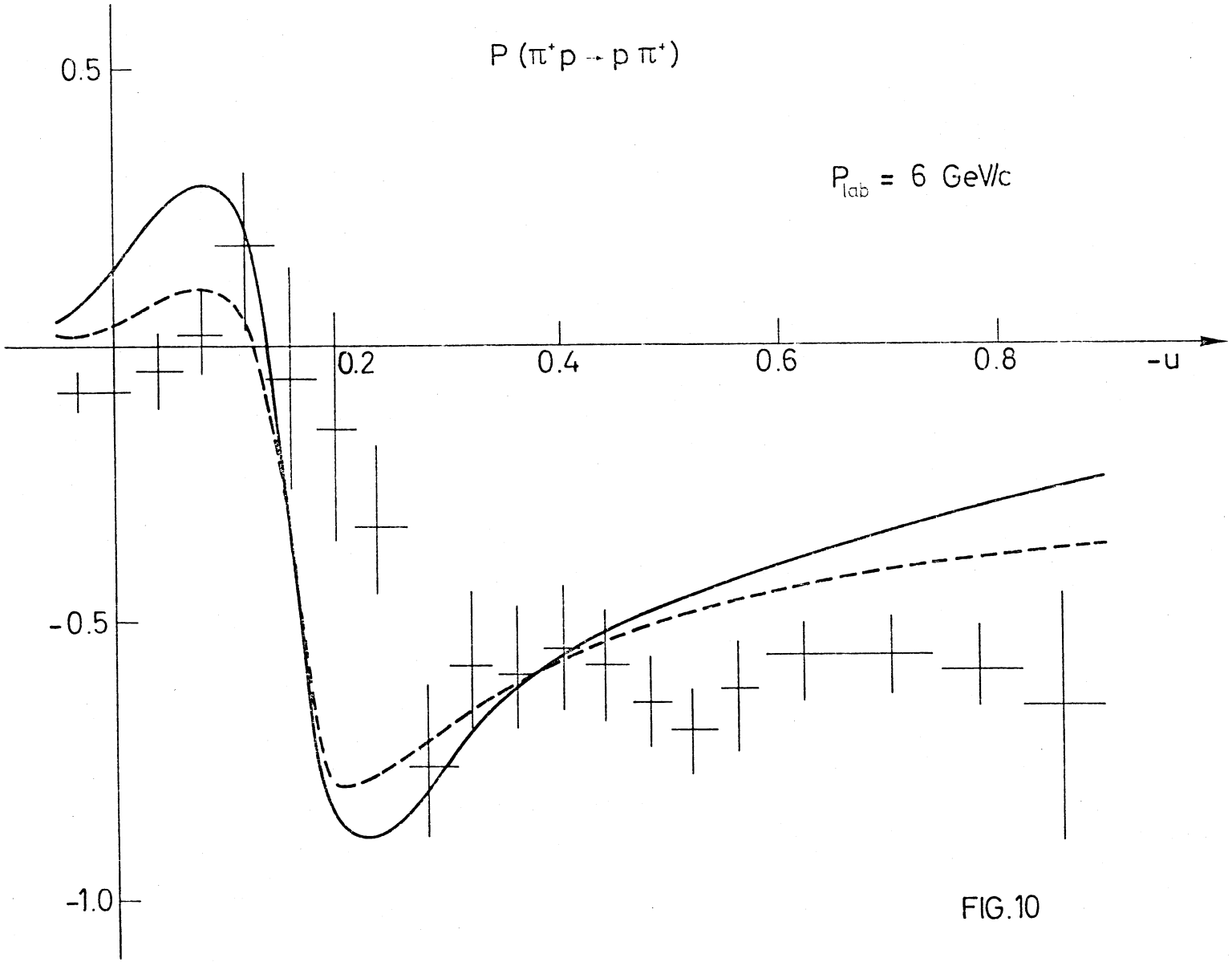

FIG. 10

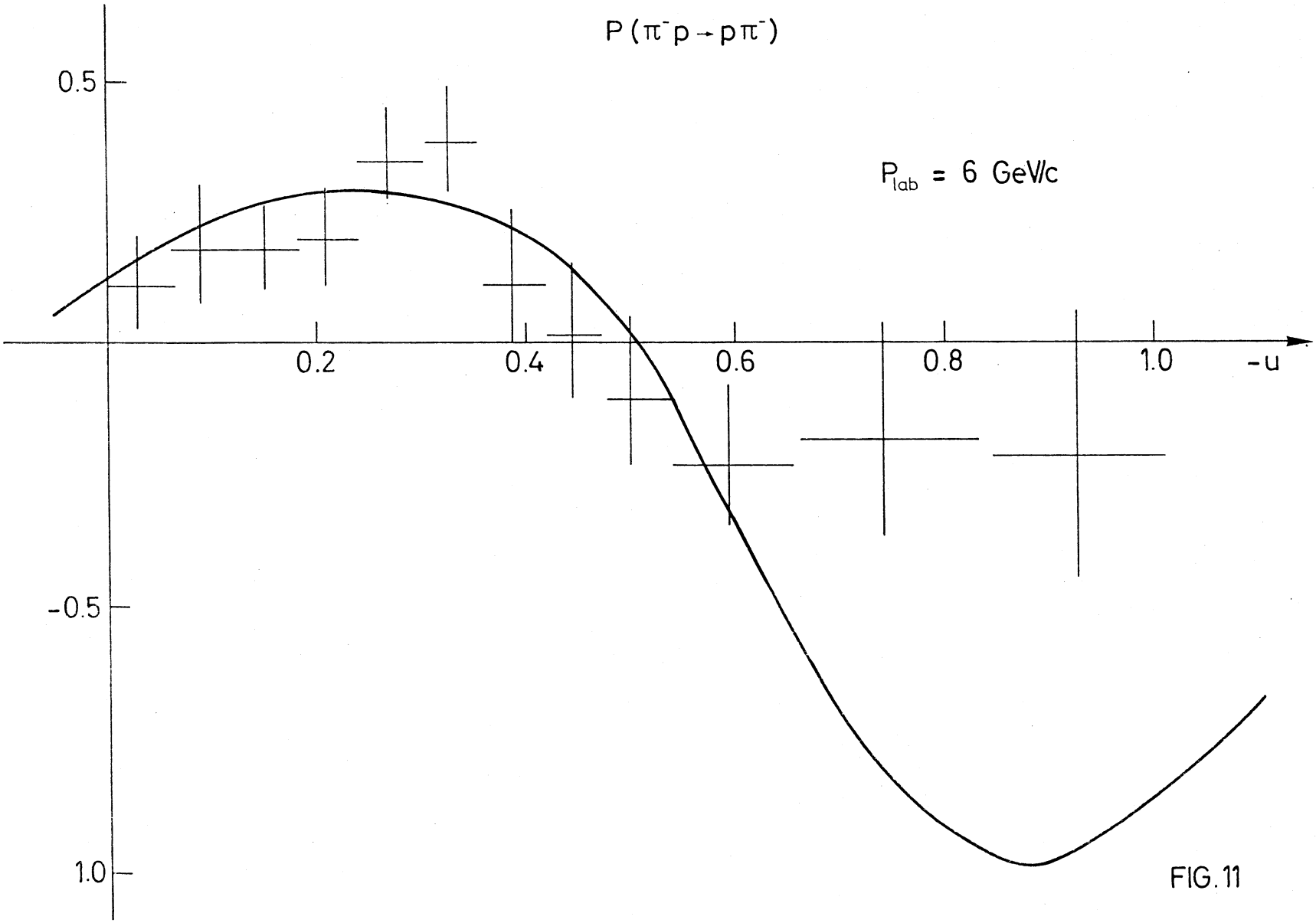

FIG. 11

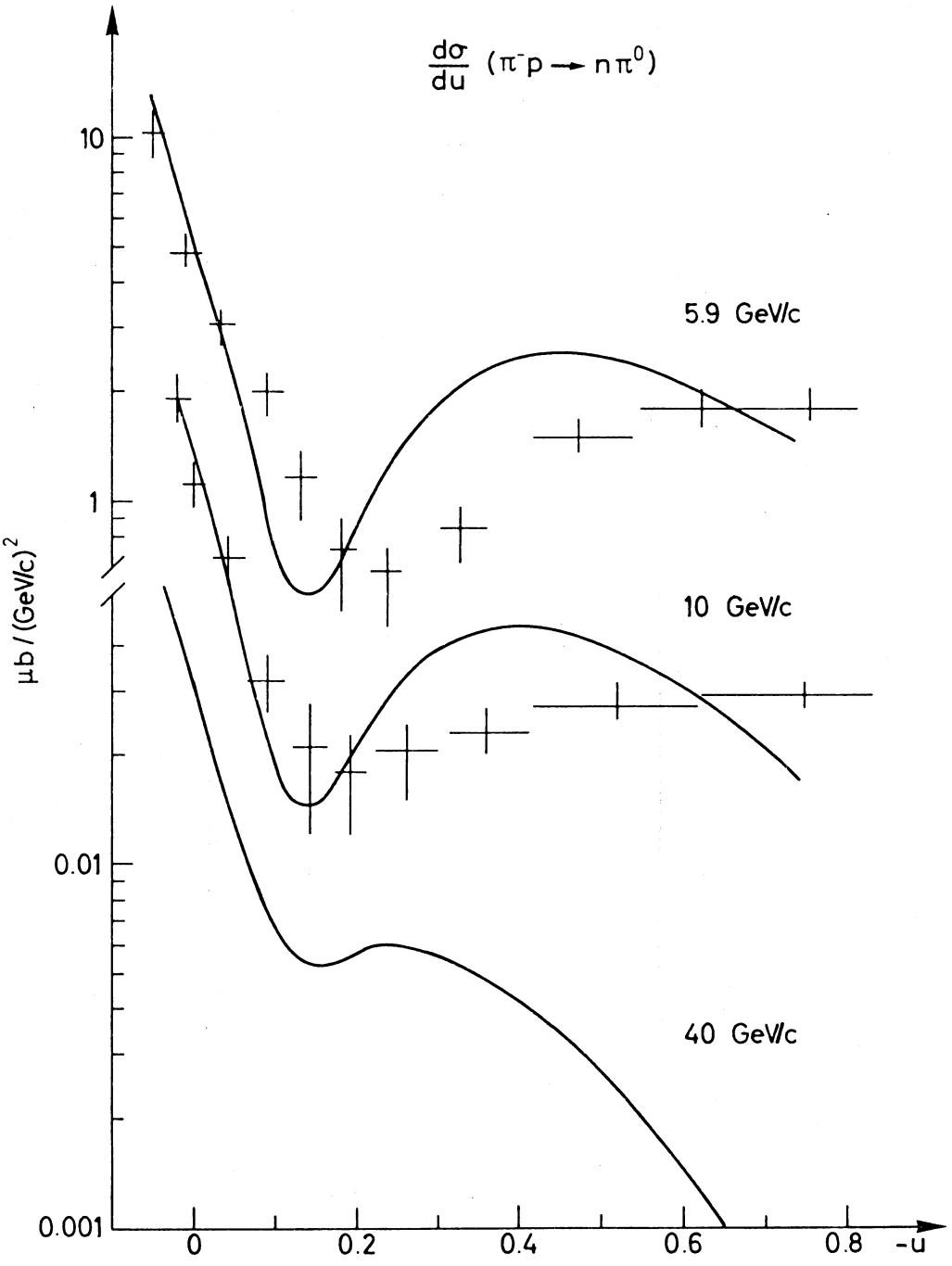
dσ/du (π⁻p → nπ⁰)
10
1
0.01
0.001
μb/(GeV/c)²
5.9 GeV/c
10 GeV/c
40 GeV/c
0
0.2
0.4
0.6
0.8
-u

Fig.12

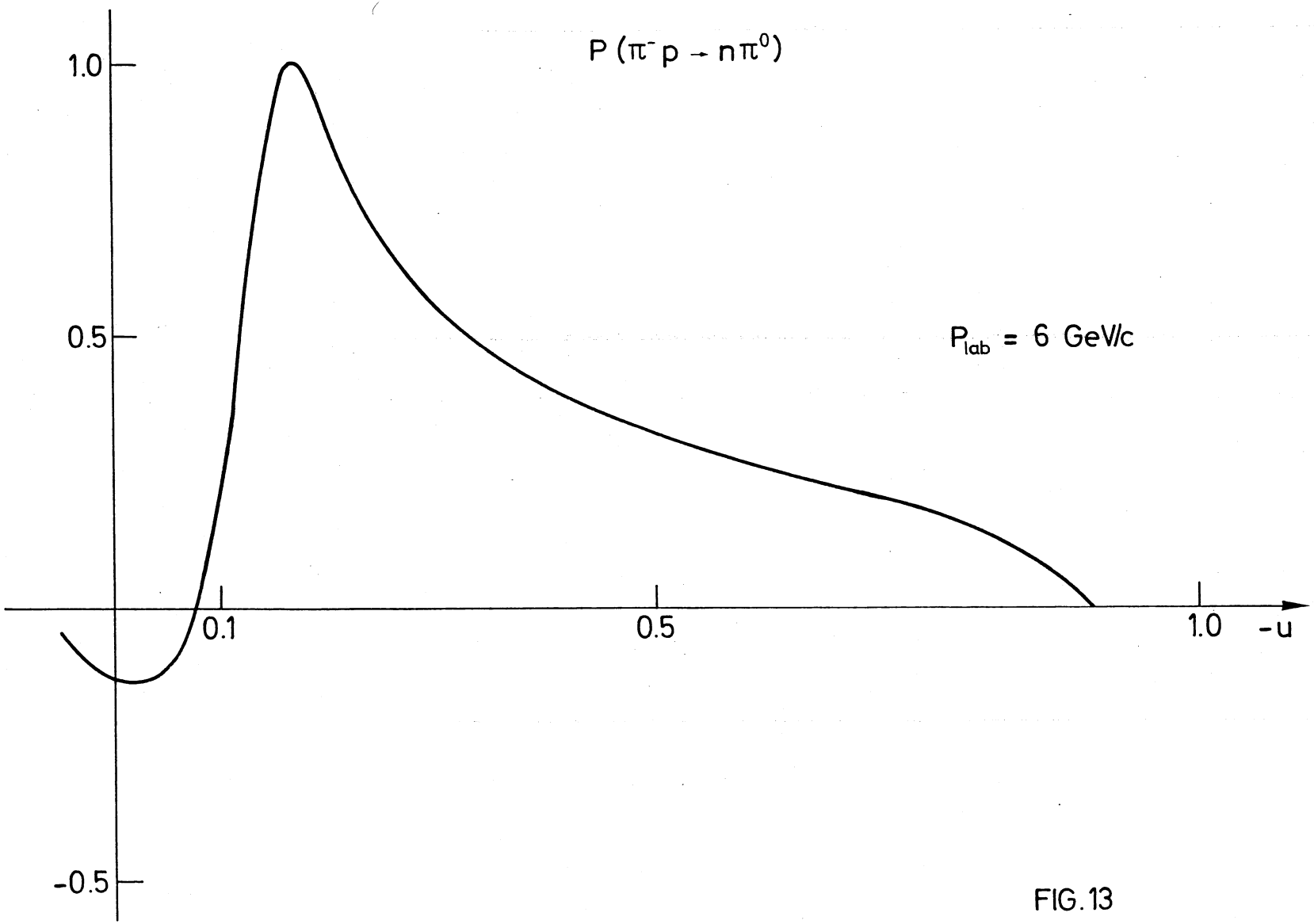

FIG. 13

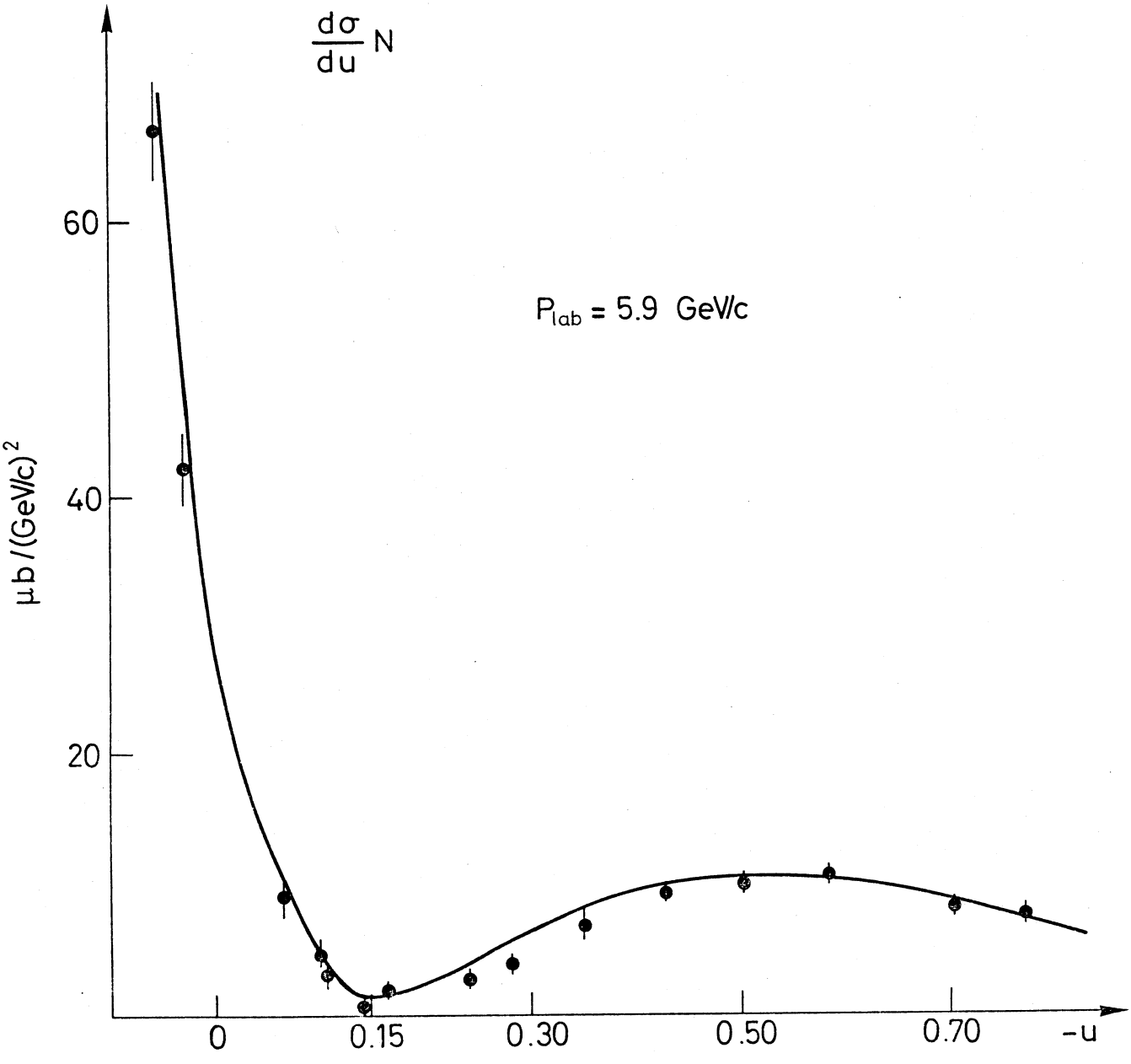

FIG.14

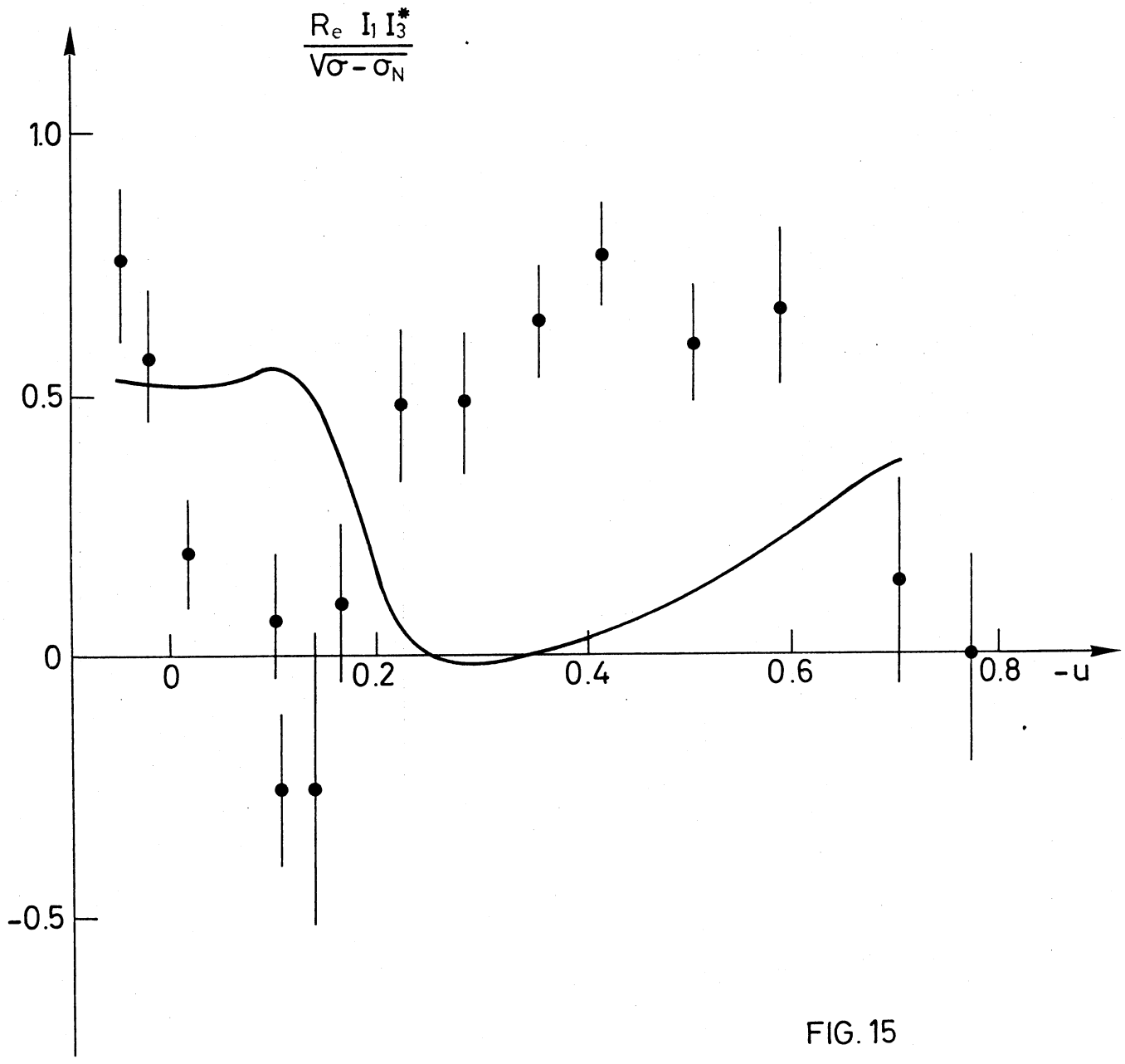

FIG. 15

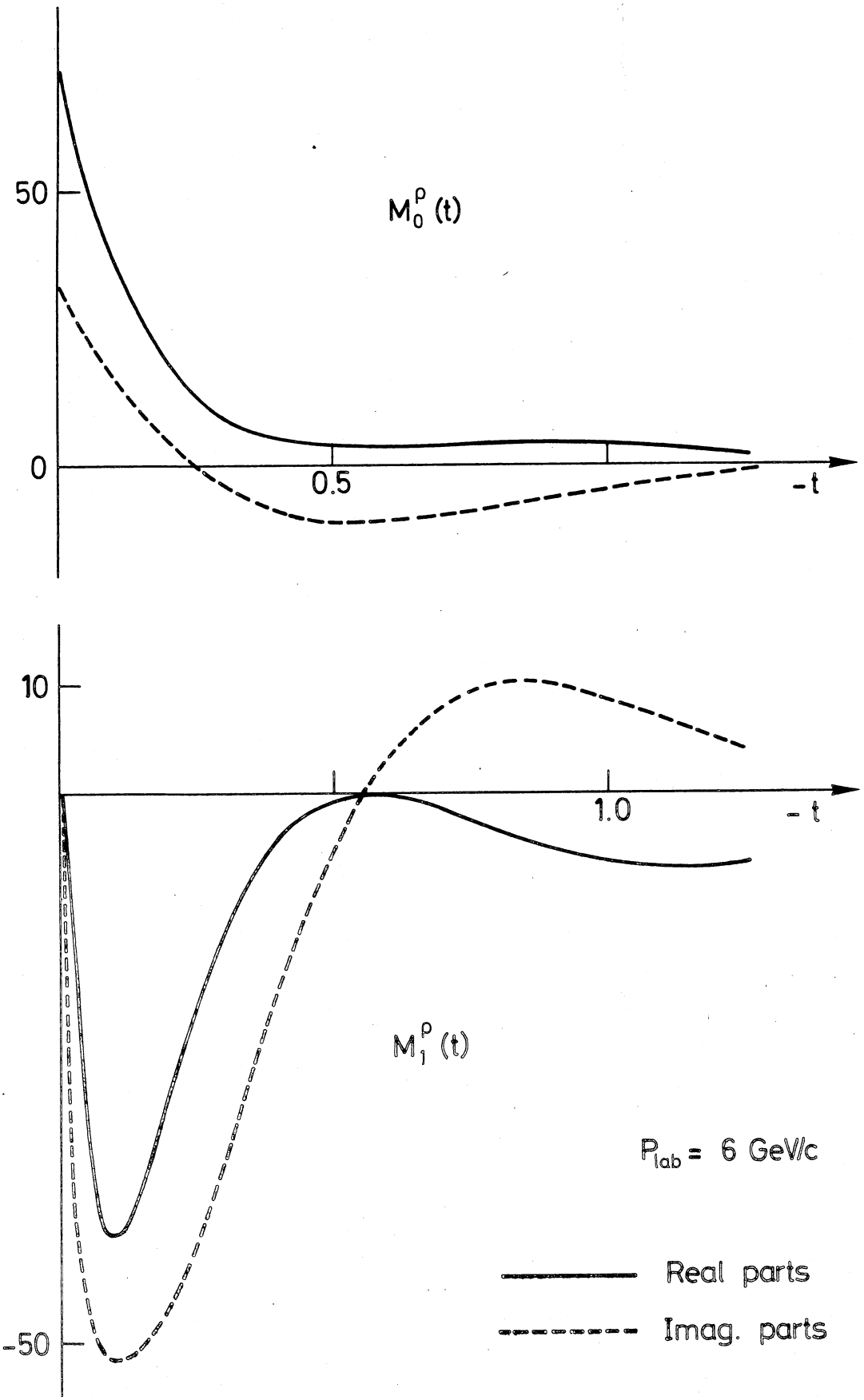

FIG. 16

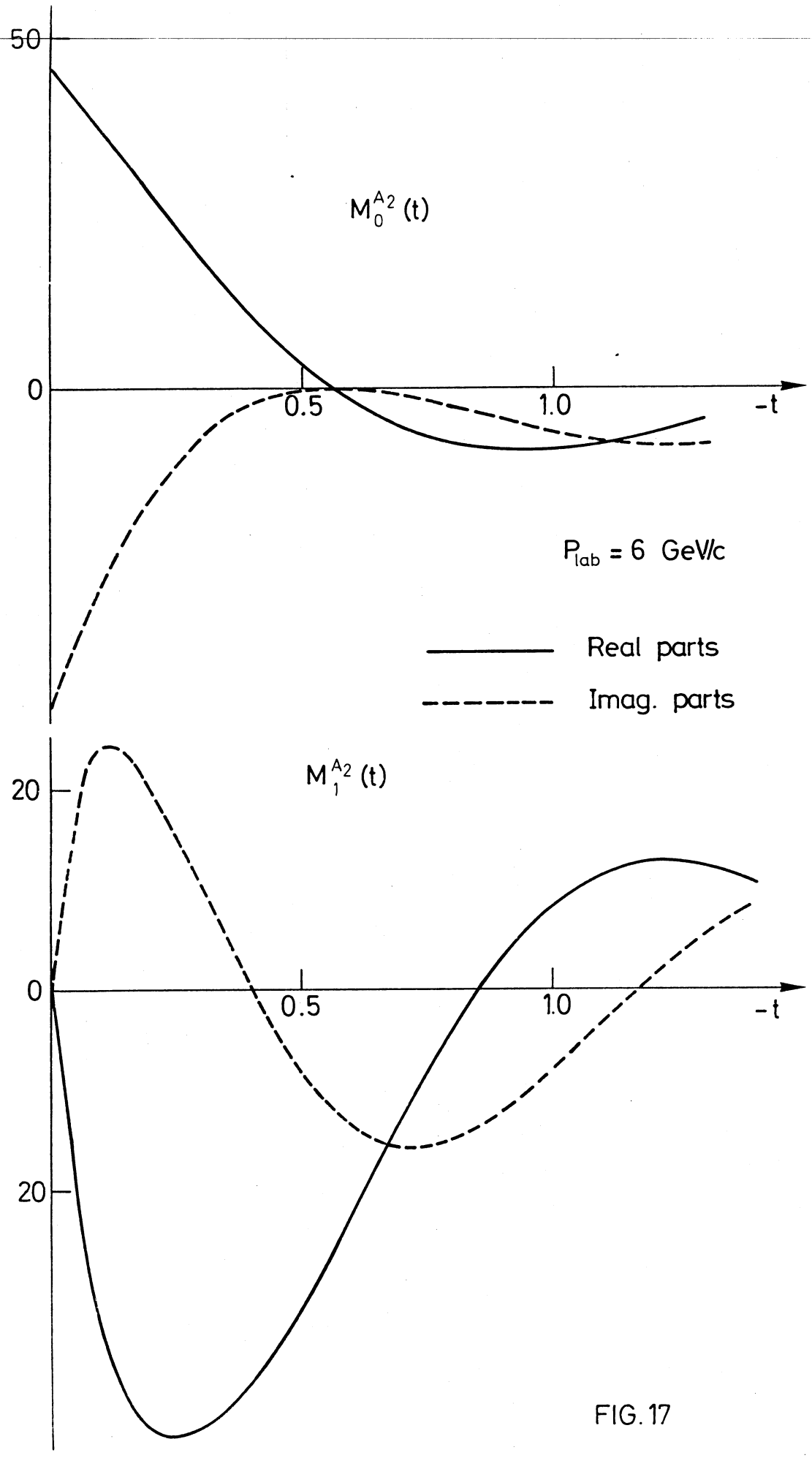
50
0
0.5
1.0
-t
M_0^{A2} (t)
P_{lab} = 6 GeV/c
Real parts
Imag. parts
20
0
20
0.5
1.0
-t
M_1^{A2} (t)

FIG. 17

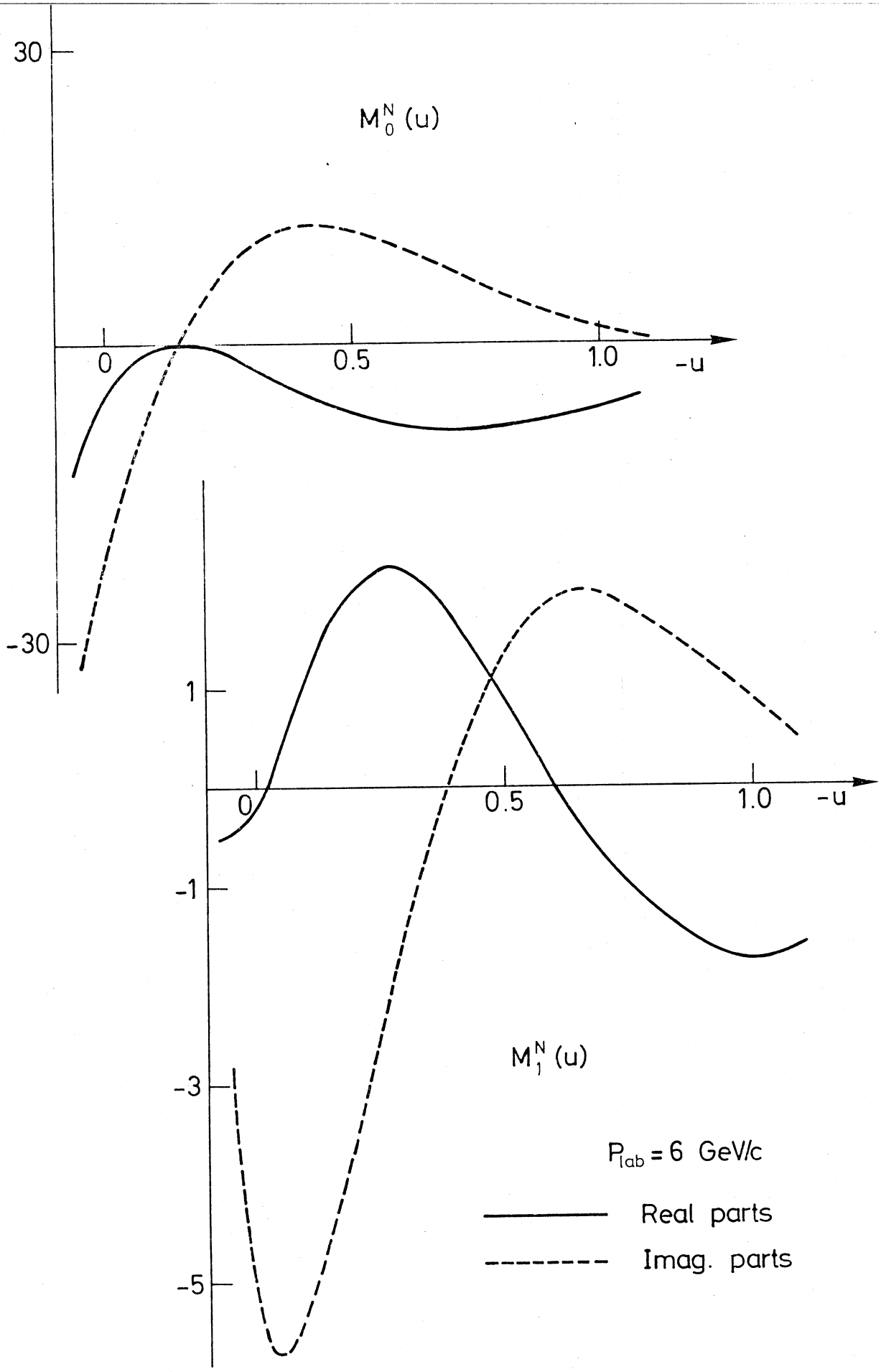
30
$M_0^N(u)$
0
0.5
1.0
-u
-30
1
0
0.5
1.0
-u
-1
-3
-5
$M_1^N(u)$
$P_{lab} = 6$ GeV/c
Real parts
Imag. parts

FIG.18

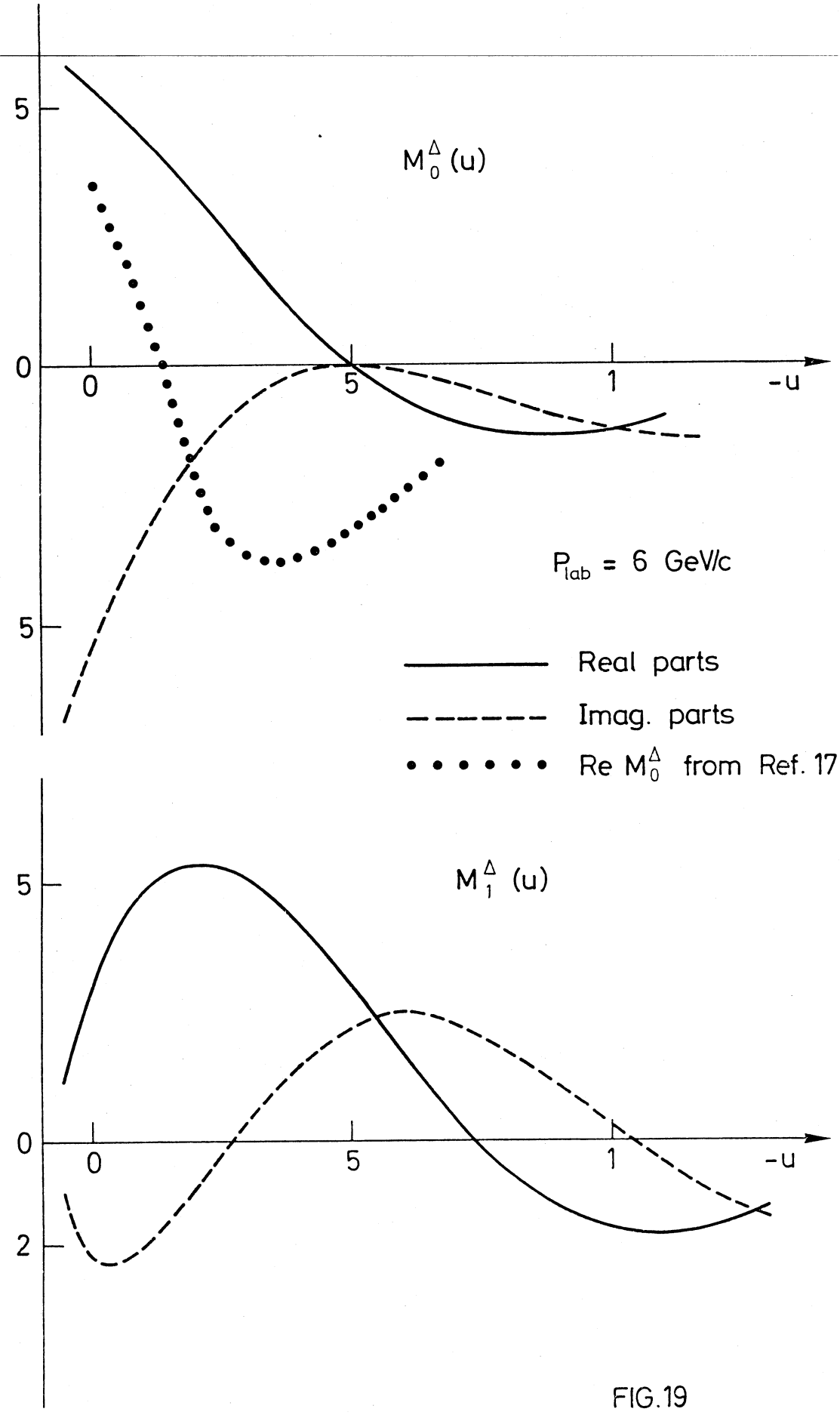
5
0
5
0
5
1
-u
$M_0^{\Delta}(u)$
P_{lab} = 6 GeV/c
Real parts
Imag. parts
Re M_0^{Δ} from Ref. 17
5
0
2
0
5
1
-u
$M_1^{\Delta}(u)$

FIG. 19

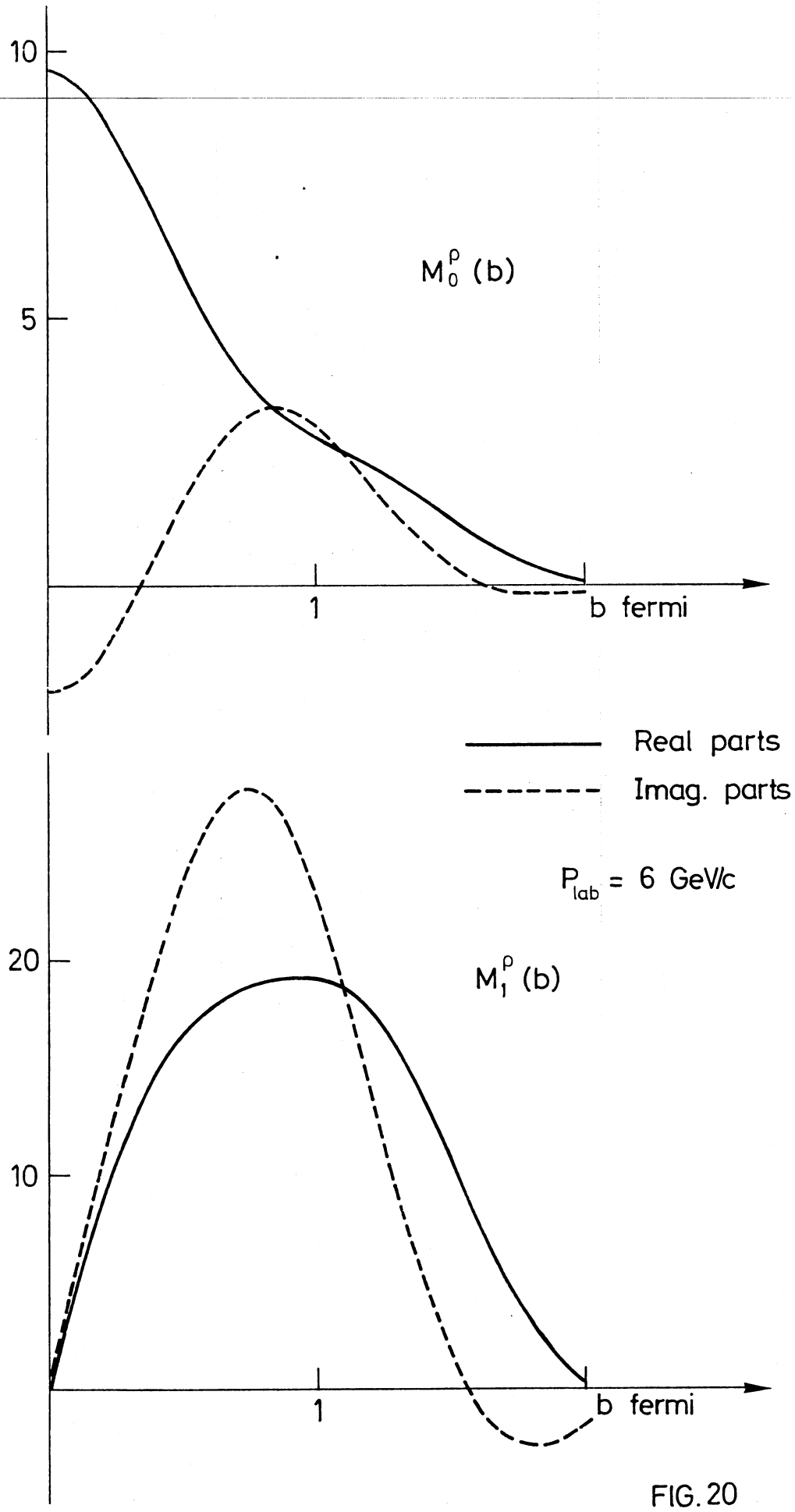
10
5
M_0^ρ (b)
1
b fermi
Real parts
Imag. parts
P_{lab} = 6 GeV/c
20
10
M_1^ρ (b)
1
b fermi

FIG. 20

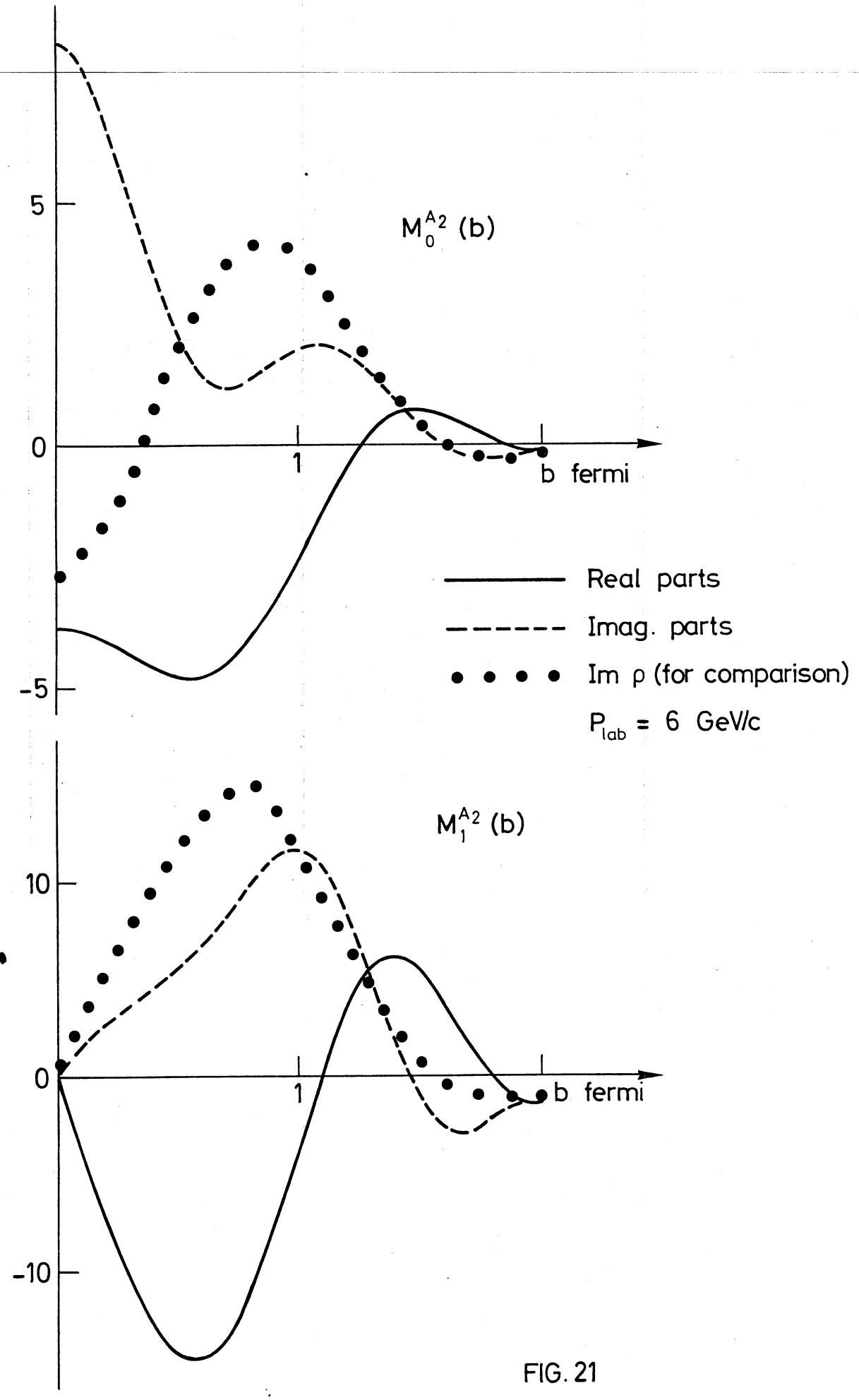
5
0
-5
1
b fermi
M_0^{A2} (b)
Real parts
Imag. parts
Im ρ (for comparison)
P_{lab} = 6 GeV/c
10
0
-10
1
b fermi
M_1^{A2} (b)

FIG. 21

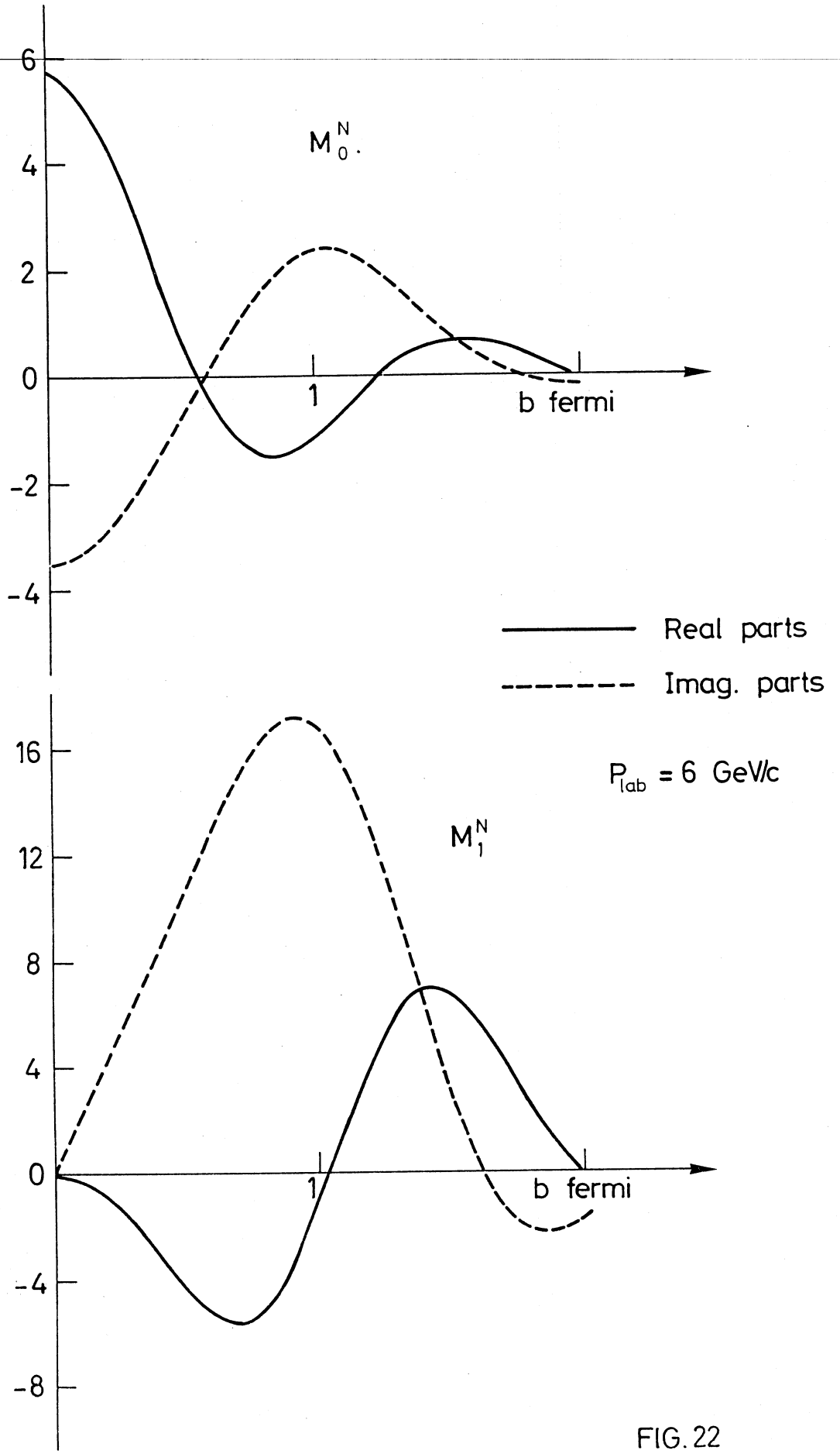
6
4
2
0
-2
-4
M_0^N.
1
b fermi
Real parts
Imag. parts
P_{lab} = 6 GeV/c
16
12
8
4
0
-4
-8
M_1^N
1
b fermi

FIG. 22

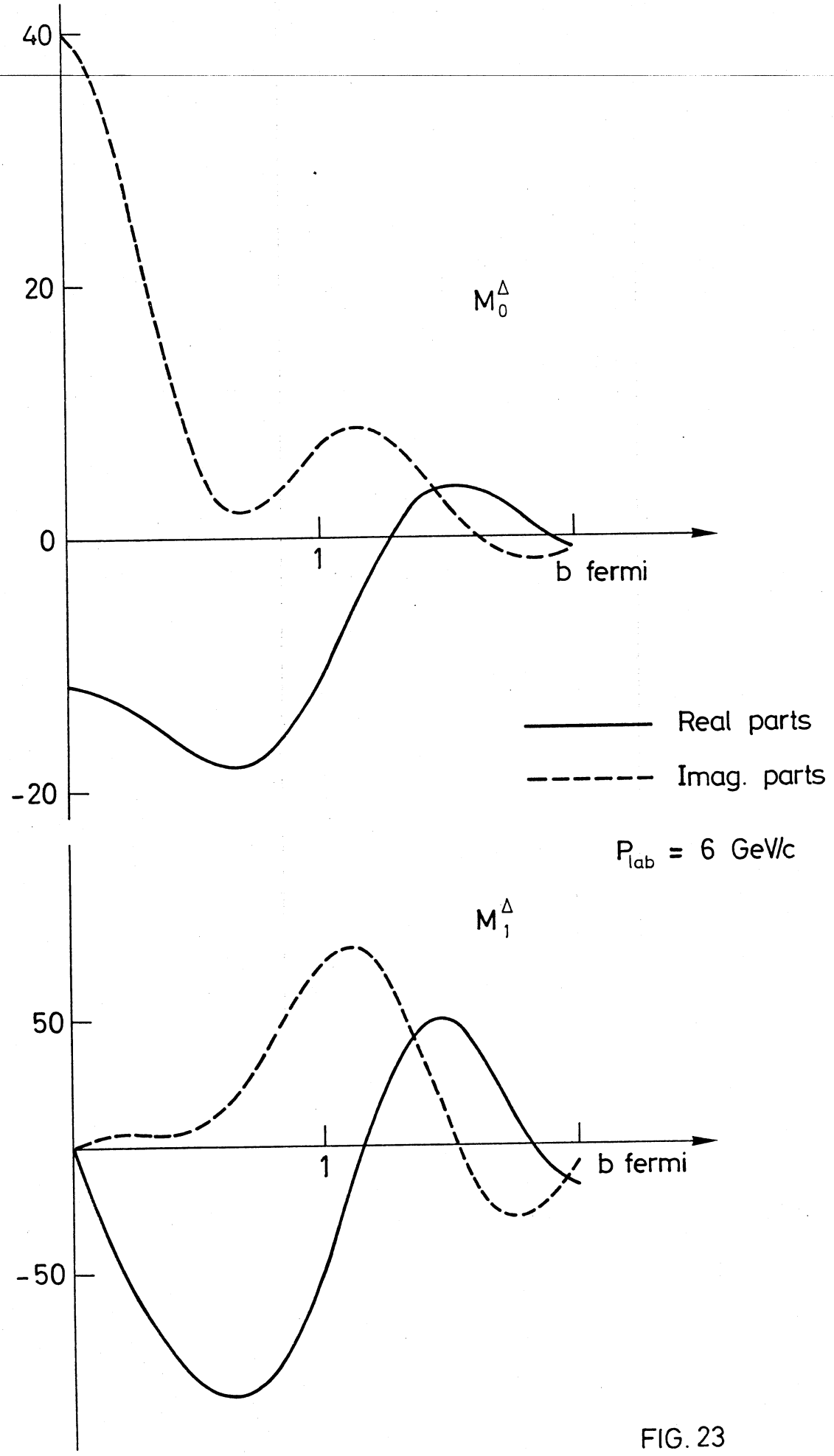
40
20
0
-20
M_0^Δ
1
b fermi
Real parts
Imag. parts
P_{lab} = 6 GeV/c
M_1^Δ
50
-50
1
b fermi

FIG. 23